

Changes in water-use strategies and soil water status of degraded poplar plantations in water-limited areas

Junjie Dai ^{a,b,c}, Ying Zhao ^{a,b,c}, Katsutoshi Seki ^d, Li Wang ^{a,b,e,*}

^a State Key Laboratory of Soil Erosion and Dryland Farming on the Loess Plateau, the Research Center of Soil and Water Conservation and Ecological Environment, Chinese Academy of Sciences and Ministry of Education, Yangling, Shaanxi 712100, China

^b Institute of Soil and Water Conservation, Chinese Academy of Sciences and Ministry of Water Resources, Yangling, Shaanxi 712100, China

^c University of Chinese Academy of Sciences, Beijing 100049, China

^d Natural Science Laboratory, Toyo University, Bunkyo-ku, Tokyo 112-8606, Japan

^e Institute of Soil and Water Conservation, Northwest A&F University, Yangling 712100, China

ARTICLE INFO

Handling editor: Dr. B.E. Clothier

Keywords:

Forest degradation

Stable isotope

Sap flow

Root water uptake

Water-use efficiency

ABSTRACT

Poplar plantations play an active role in windbreak and sand-fixation and timber production in water-limited areas, but the large-scale plantations are experiencing degradation, characterized by short trees, small size, and dieback. Moreover, the potential impacts of plantation degradation on ecohydrological processes in soil-plant systems remain unclear. We continuously measured soil water content (SWC), hydrogen and oxygen isotopic compositions in the soil water and plant xylem water, carbon isotopic compositions in the leaf, and sap flow velocity of poplar trees under various degraded plantations (no degraded, ND; lightly degraded, LD; severely degraded, SD) during the 2021 growing season (May–September). We also investigated tree root systems at a depth of 0–200 cm. Our results showed that as plantation degradation intensified, the root weight density at different depths decreased and the root proportion of the shallow layer (0–40 cm) increased. Although the SWC of the shallow layer did not change in the degraded plantations, the SWCs at middle layer (40–80 cm) and deep layer (80–200 cm) were higher in the LD and SD plantations than in the ND plantations, which might be related to reduced transpiration of degraded plantations. The Bayesian mixing model showed that all plantations can shift the water source from shallow to deep layers in the process of soil wetting to drying. Evidence from leaf carbon isotopes suggested that degraded plantations increased the sensitivity of intrinsic water-use efficiency to SWC. Our findings demonstrate that the normal growth of poplar plantations is prone to soil desiccation of deep layers due to high transpiration demand in water-limited areas, and degraded poplar plantations alleviate deep soil water depletion due to low transpiration. For rain-fed poplar plantations, proper thinning and measures of reducing soil evaporation may be necessary to avoid water excess consumption from deep soils.

1. Introduction

Forests account for approximately 45% of global terrestrial carbon storage, play an essential role in the water cycle of terrestrial ecosystems, and provide various critical ecosystem services for maintaining biodiversity (Choat et al., 2018; Liu et al., 2021). However, global warming has increased the frequency of regional drought events and increased the duration and intensity of droughts (Allen et al., 2010), especially in arid and semi-arid areas (Iqbal et al., 2021). These changes have led to decreased water availability and soil degradation in forests and reduced biodiversity in the affected areas, reducing the forest area. In efforts to increase the carbon sink, enhance biodiversity, and prevent

wind and soil erosion in water-limited areas, afforestation projects have been implemented worldwide (Chen et al., 2019; Yang et al., 2022), especially in China (Guo, 2021; Su and Shangguan, 2019). China accounted for 6.6% of the vegetation area worldwide but contributed 25% of the global net increase in leaf area from 2000 to 2017, contributing to global greening efforts (Chen et al., 2019).

Afforestation is a challenging task in areas with little precipitation. The vegetation carrying capacity of the local soil water status and appropriate afforestation species should be considered. Unfortunately, an increasing number of studies have found that water-limited regions are observing widespread degradation of plantations, which are characterized by short height, small size, and dieback (Chen et al., 2015; Liu

* Correspondence to: Institute of Soil and Water Conservation, Chinese Academy of Sciences and the Ministry of Water Resources, Yangling 712100, China.
E-mail address: wangli5208@nwafu.edu.cn (L. Wang).

et al., 2020; McVicar et al., 2010; Sun et al., 2018; Zhang et al., 2020). A key factor contributing to this problem is insufficient water (Liu et al., 2021). Thus, improving the understanding of how silvicultural species adapt to adversity and directing future silvicultural practices toward sustainable development requires focusing on how these degraded plantations modify their water-use strategies.

Degraded plantations might have a low transpiration rate owing to the small tree size and narrow canopy width; moreover, they might lose the ability to use deep soil water because of the shallow root systems (Liu et al., 2021). Because the availability of deep-water sources often enables trees to eliminate drought stress (Brinkmann et al., 2016; Ding et al., 2021), trees in degraded plantations with low deep-root activity may be vulnerable to drought (Liu et al., 2021). Most studies have suggested that plantation degradation is associated with low availability of soil water in the root zone (Liu et al., 2021; Sun et al., 2018; Zhang et al., 2020). Jia et al. (2017) reported a decrease in soil water storage and even severe soil desiccation at the deep soil layer due to afforestation across the Chinese Loess Plateau. Soil desiccation of the deep layer makes it difficult for plantations to extract water from the root zone. Under soil drought conditions, trees often suffer from reduced photosynthetic carbon sequestration and non-structural carbohydrate depletion (McDowell et al., 2008), which might stunt plantation growth.

Recently, stable isotopes (^2H , ^{18}O , and ^{13}C) have been extensively used in critical eco-hydrology topics, such as determining the spatio-temporal sources of the water that plants uptake (Miguez-Macho and Fan, 2021), calculating the mean transit time of various hydrological components (Dai et al., 2022), estimating the source water contribution to root water uptake (Dai et al., 2020a), and analyzing the intrinsic water-use efficiency (WUE_i) of a plant (Wu et al., 2022). Many studies have investigated the sources of water utilization in silvicultural vegetation, including the same species in mixed and pure forests (Tang et al., 2018), different species in mixed forests (Dai et al., 2023c; Grossiord et al., 2014), different types of pure forests (Wang et al., 2020), and different plantation ages (Wang et al., 2021). However, few researchers compare the water-use strategies of trees between degraded and normal plantations. Filling these knowledge gaps will help clarify the mechanisms of plantation degradation and provide a scientific basis for plantation management in semi-arid regions.

Generally, the species in afforestation in water-limited areas have strong drought adaptability and can regulate water-use strategies under changing water conditions. For instance, from the rainy season to the dry season, drought-tolerant species can shift the water source from the shallow soil layer to the deep soil layer through dimorphic roots (Wang et al., 2017), increase the WUE_i (Wang et al., 2021), or adopt isohydric behavior to reduce water loss (Ding et al., 2021). Although seasonal patterns in deep soil water utilization help trees survive drought, they also accelerate the depletion of deep soil reservoirs, reducing the stability of plantations in water-limited areas (Chen et al., 2008; Liu et al., 2021; Su and Shangguan, 2019). Because precipitation may have been consumed by soil evaporation and vegetation transpiration before infiltrating into the deep layer, deep water sources do not replenish quickly. Notably, assessing the soil water-carrying capacity for vegetation and guiding water management in water-limited areas requires understanding the relative contributions of different water sources and the absolute water consumption of plantations. Water consumption from soil water storage can be calculated by coupling stable isotopes with the thermal dissipation method (Granier, 1987), enabling a comprehensive understanding of the relationship between forest and water and preventing further plantation degradation.

This study was conducted on poplar plantations in a semi-arid area of the Chinese Loess Plateau. Poplar trees (*Populus simonii* Carr.) are the local vanguard species for afforestation projects; however, extensive tree degradation and even mortality have been occurring in these plantations. First, we conducted a field investigation measuring tree growth indicators (height, size, canopy width, and dead branches) and then conducted a comprehensive evaluation to distinguish the degradation

degrees of plantations. Next, the soil water content, hydrogen and oxygen isotopic compositions in the soil water and xylem water, carbon isotopic compositions in the leaf, and sap flow of trees were continuously measured at each sample site during the growing season. The objectives were to: (1) identify the isotopic characteristics of soil water, xylem water, and leaves, (2) compare the water-use strategies (transpiration, root water uptake patterns, and WUE_i) under different categories of degradation, and (3) elucidate the links between poplar plantations and soil water status. We hypothesized that (1) with increased plantation degradation, the deep roots and transpiration will decrease, and (2) degraded plantations reduce the relative contribution and absolute use of deep soil water and alleviate deep soil water depletion.

2. Materials and methods

2.1. Study area and sampling sites

This study was conducted at the Shenmu Erosion and Environment Experimental Station of the Chinese Academy of Sciences in the Liudaogou catchment of the Loess Plateau, China ($110^\circ 21'E$, $38^\circ 47'N$), and has an area of 6.9 km^2 (Fig. 1a). The area is in an interlaced zone that experiences wind and water erosion and constitutes the transition from the hilly loess area to Mu Us Desert. The catchment is a typical loess hilly landform with sand cover; belongs to a middle-temperate semi-arid climate zone; and, from 2003 to 2017, had an average annual temperature of 8.4°C and annual precipitation of 459 mm. The total precipitation for the observation year (2021) was 330.9 mm, of which 69.7% occurred during the plant growing season (May to September). Daily temperature in 2021 ranged from -20.2 – 28.7°C , with an average of 10.2°C . Daily relative humidity in 2021 ranged from 13.0% to 99.8% with an average of 46.9%. Frequent sandstorms and intense wind erosion occur in spring, and rainstorms resulting in strong water erosion (i.e., interrill and gully erosion) occur mostly in summer.

The sampling sites were on flat sandy land at the southern end of the Liudaogou catchment at an altitude of 1198 m and a slope of $<2^\circ$. The soil texture was sandy (USDA classification), and the granular composition was 95.7% sand, 3.2% silt, and 1.1% clay. The field capacity and wilting coefficient of the soil were 0.084 and $0.008 \text{ cm}^3 \text{ cm}^{-3}$, respectively. The vegetation was dominated by planted poplar trees ($\sim 800 \text{ tree ha}^{-1}$), with a planting area of $\sim 150\,000 \text{ m}^2$.

2.2. Determination of sampling sites to reflect different categories of degradation

Poplar plantations on the sandy land were surveyed in early May 2021 to establish long-term sampling sites. Our literature review and consultations with local farmers demonstrated that poplar plantations were built in the study area in approximately 1999. The degradation degree of poplar plantations was investigated in detail according to the growth status and spike top (Liu et al., 2020, 2021). The “spike top” was described as a dead area of the trunk in the upper canopy of poplar trees showing continuous growth of lateral branches (Fig. 1c).

First, we determined three $50 \times 50 \text{ m}^2$ sites with distinct growth differences in height, size, canopy width, and spike top (Fig. 1b). Their microtopography, climate, and soil texture were similar, and poplar plantations in the three sites experienced varying degrees of degradation after similar years of growth. Next, four $20 \times 20 \text{ m}^2$ plots were established in each site, and the growth indicators of all poplar trees were measured, namely, the tree height, spike top height, diameter at breast height (DBH), and canopy projection area (A_c , calculated by the crown width in the east-west and north-south directions). The canopy density of each plot was obtained from the ratio of total A_c to total area. We surveyed 128 trees at each site. The data is shown in Table 1.

Notably, in one of the three sites, poplar trees had the best growth according to the growth indicators and no dead branches on the main

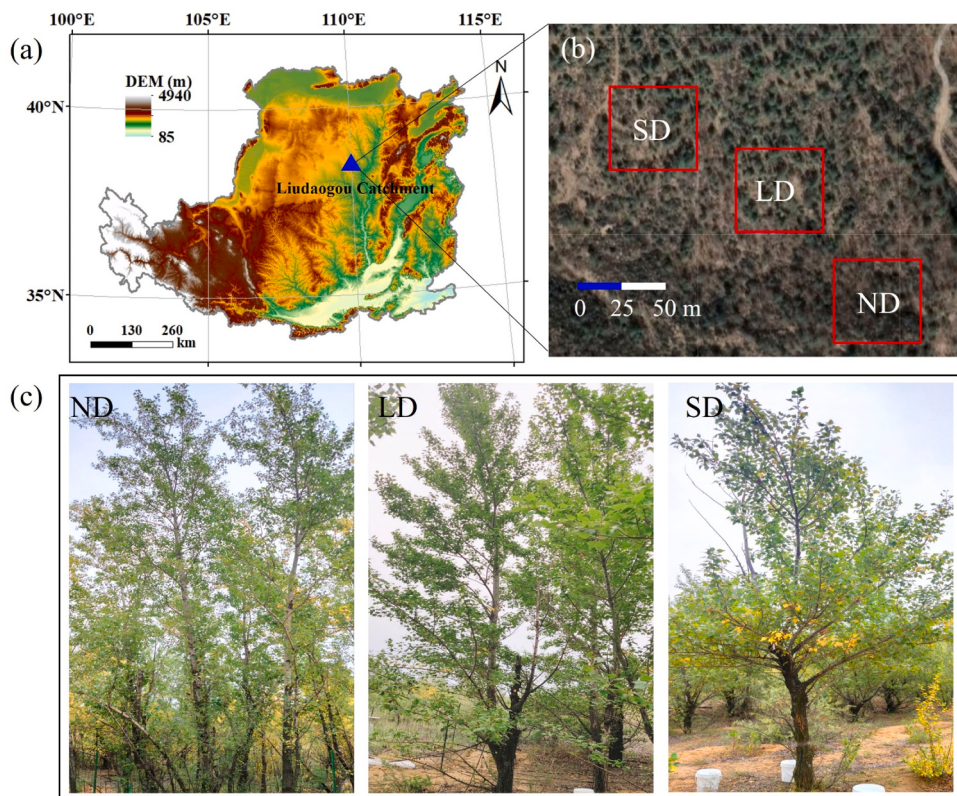


Fig. 1. Geographical location of this study area (a), location of sampling sites (b), and growth status of poplar trees (c). The satellite image in Fig. (b) is from <https://www.earthol.com/g/>; the red areas represent fixed sampling sites. ND, LD, and SD indicate no, lightly, and severely degraded plantations, respectively.

Table 1
Basic characteristics of poplar plantations at different sampling sites.

Growth status	Tree height (m)	Spike top height (m)	Spike top ratio (%)	DBH (cm)	A _c (m ²)	Crown density (%)
ND	10.3 ± 1.3a	0b	0c	19.2 ± 3.8a	10.3 ± 3.4a	83.4 ± 13.2a
	9.3 ± 1.0a	2.6 ± 0.4a	28.0 ± 3.5b	15.4 ± 2.1b	9.0 ± 1.9a	72.0 ± 9.5a
LD	5.9 ± 0.8b	2.7 ± 0.3a	45.8 ± 3.1a	12.5 ± 1.6c	5.9 ± 1.5b	47.2 ± 8.4b
	5.9 ± 0.8b	2.7 ± 0.3a	45.8 ± 3.1a	12.5 ± 1.6c	5.9 ± 1.5b	47.2 ± 8.4b

ND, LD, and SD indicate no, lightly, and severely degraded plantations, respectively. The DBH and A_c represent diameter at breast height and canopy projection area, respectively. Values are shown as the mean ± standard deviation. The number of samples (*n*) was 128 for the tree growth indicators, except for canopy density (*n*=4). Different lowercase letters indicate significant differences in tree morphological indicators among different sampling sites (*P*<0.05), based on the Tukey HSD post hoc test in one-way ANOVA.

trunk (Fig. 1c); this site was defined as no degraded (ND) plantations. The mean tree height, DBH, and A_c in the ND plantations were 10.3 m, 19.2 cm, and 10.3 m², respectively (Table 1). However, the growth status of poplar plantations in the other two sites was lower than that in the ND plantations to varying degrees, and the poplar trees exhibited a spike top. According to the criteria employed in the literature (Liu et al., 2020, 2021), we defined the site with an average spike top ratio of 0–40% as lightly degraded (LD) plantations, and an average spike top ratio of more than 40% as severely degraded (SD) plantations. The spike top ratio was derived by dividing the average spike top height by the average tree height at each site. The DBH and spike top ratio of poplar trees were significantly (*P*<0.05) smaller and greater, respectively, in the LD plantations than in the ND plantations (Table 1). Poplar trees in the SD plantations had the worst growth parameters, with an average

height, DBH, and A_c of 5.9 m, 12.5 cm, and 5.9 m², respectively (Table 1).

2.3. Sampling and isotope analysis

From May to September 2021, soil and plant samples were collected monthly from three fixed sites of 20 × 20 m² characterized as ND, LD, and SD. The specific sampling dates were May 24, June 28, July 28, August 27, and September 24. Because the variability in tree morphology appeared mainly among the sampling sites with different categories of degradation rather than within the same site (Table 1), we selected three sample trees at each fixed site and three soil profiles for isotopic sampling; these sample trees had morphological indicators similar to the average of the trees of each site in Table 1. For the xylem samples, three lignified twigs (~1.5 cm in diameter) at a height of 200 cm were collected from the south-facing side of three sample trees. The twigs were peeled, sealed in a 12 mL glass bottle with parafilm, and transported to the laboratory for frozen storage. Mature and healthy leaves in the upper layer of the canopy under no shading conditions were also collected from these sample trees (three replicate leaf samples). Fresh leaves (~40 g) were then packed in paper bags and transported to the laboratory for pretreatment, which comprised drying at 75°C for 48 h in an electric heating air-blowing drier, grinding to pass through an 80-mesh screen, and sealing in a polyethylene bag for preservation at 15°C. We collected three xylem and leaf samples at each site on each sampling date; 45 xylem samples and 45 leaf samples were collected during the observation period.

Soil samples were obtained using a hand drill (40 mm in diameter) at 1.5 m from the sample trees (three replicates per degradation class). The sampling depth was 0–200 cm. The sampling intervals were 10 and 20 cm at the depth of 0–20 cm and below 20 cm, respectively. We collected 33 soil samples at each site on each sampling date; 495 soil samples were collected during the observation period. The samples were

divided into two parts. One part was oven-dried to measure the soil gravimetric water content. The other part was sealed into a 12 mL glass bottle with parafilm and transported to the laboratory for frozen storage. A cryogenic vacuum distillation system (Li-2100, LICA Inc., Beijing, China) was employed to extract water from the xylem and soil, and the water extraction efficiency was over 99%. For the specific operational processes, see Zhao et al. (2021).

In August 2021, a root investigation of poplar trees was conducted using a root drill (90 mm in diameter) in the 0–200 cm soil profile. One sample tree trunk was selected as the origin in the ND, LD, and SD sites, with no shrubs and herbs nearby, and three soil cores at a depth of 0–200 cm were collected from 50, 100, and 200 cm from the trunk in a southerly direction. The sampling interval was the same as that used for the soil samples. Each soil layer was passed through a screen (2 mm in diameter) for root-soil separation. Fine roots (<2 mm in diameter) were sealed in polyethylene bags for preservation, and the root weight density was determined using the oven-drying method.

Daily-scale precipitation samples and the precipitation amount were obtained from May to September 2021 ($n=15$) by using a rain gauge placed on the open ground ~1000 m from the sampling sites. Because light rainfall events (precipitation <3 mm in one event) only moistened a few centimeters of soil in the poplar plantation, we collected precipitation samples in 30 mL polyethylene bottles after each rainfall event with precipitation >3 mm, immediately sealed them with parafilm, and transported them to the laboratory for frozen storage. Notably, each rainfall event could not have more than 4 h of consecutive precipitation-free periods. If there were multiple rainfall events in 1 d, their samples were combined into one precipitation sample.

The hydrogen and oxygen isotopic compositions of the precipitation and soil water were analyzed using a liquid-water isotopic analyzer (912-0032, LGR Inc., California, USA). The hydrogen and oxygen isotopic compositions of xylem water were analyzed using a stable isotope ratio mass spectrometer (Isoprime-100, Isoprime Inc., Cheadle, UK) to avoid spectral pollution. Cross-testing the same set of LGR4E standard water samples (manufactured by LGR Inc., USA) with the two devices yielded identical results. The carbon isotopic compositions of leaf samples were analyzed using the stable isotope ratio mass spectrometer (solid sample testing mode). Isotopic compositions are expressed using delta notation as follows:

$$\delta X(\text{‰}) = R_{\text{sample}}/R_{\text{standard}} - 1 \quad (1)$$

where δX represents the $\delta^2\text{H}$, $\delta^{18}\text{O}$, and $\delta^{13}\text{C}$, and R_{sample} and R_{standard} are the isotopic ratios of the measured and standard samples (${}^2\text{H}/{}^1\text{H}$, ${}^{18}\text{O}/{}^{16}\text{O}$, and ${}^{13}\text{C}/{}^{12}\text{C}$, respectively). The standard samples were Vienna Standard Mean Ocean Water for $\delta^2\text{H}$ and $\delta^{18}\text{O}$ and Pee Dee Belemnite for $\delta^{13}\text{C}$. The accuracies of $\delta^2\text{H}$, $\delta^{18}\text{O}$, and $\delta^{13}\text{C}$ were 0.5‰, 0.1‰, and 0.1‰, respectively.

2.4. Soil water content

At each sample site (ND, LD, and SD), seven soil water sensors (10HS, METER Group, Inc., Washington, USA) were installed in a 0–200 cm soil profile at a distance of ~2 m from the sample tree to continuously monitor the soil volumetric water content (SWC) at various depths (10, 20, 40, 80, 120, 160, and 200 cm) from June to September 2021. The sampling interval was 30 min. The SWC monitoring data were calibrated using the oven-drying method and cutting ring method. The calibration process was described in Dai et al. (2023b). The time series of the SWC at each depth monitored by sensors and manual measurement are shown in Fig. A1 and Fig. A2 of Appendix A, respectively, and their correlation coefficient was 0.87 ($P<0.001$, $n=210$). Because our experimental sites were on flat sandy areas and the soil texture was homogeneous (soil sand content >95%), the spatial variability of the SWC within the same site was negligible, and the continuous SWC monitoring data of one soil profile in each site can reflect the temporal variation in

SWC in the site. Moreover, the differences in SWC among the experimental sites were assumed to be related to vegetation water consumption.

Relative extractable soil water (REW) was used to evaluate the dry and wet conditions of soil by using the following formula (Iqbal et al., 2021):

$$\text{REW} = \left(\frac{\text{SWC}_{0-200} - \text{SWC}_{\min}}{\text{SWC}_{\max} - \text{SWC}_{\min}} \right) \quad (2)$$

where SWC_{0-200} is the average SWC ($\text{cm}^3 \text{cm}^{-3}$) at 0–200 cm depth, and SWC_{\min} and SWC_{\max} are the minimum and maximum average SWC at 0–200 cm depth during the growing season, respectively. The $\text{REW}<0.4$ indicates that the soil is in the dry stage, and the $\text{REW}\geq0.4$ indicates that the soil is in the wet stage (Zhou et al., 2013).

2.5. Sap flow measurements

To avoid the influence of the removal of branches on the sap flow measurement during isotopic sampling, at each sample site (ND, LD, and SD), we continuously monitored the sap flow velocity of five trees close to the soil and plant sampling sites by using a thermal dissipation probe (TDP-20, Dynamax Inc., TX, USA) 1.3 m above the ground on the north side from June to September in 2021 (poplar tree leaves fall extensively at the beginning of October). Data were recorded by loggers (CR-1000, Campbell Scientific, Utah, USA) at 30 min intervals. The height, DBH, and A_c of these sample trees were close to the mean of each sample site in Table 1. TDP-20 consisted of upper and lower probes (20 mm in length and 2 mm in diameter) containing a copper-constantan thermocouple, and the probes were used for heating and as a reference, respectively. The temperature difference (ΔT , °C) between the two probes and the maximum ΔT (ΔT_m , °C) (when the sap flow was near zero) were calculated, and the sap flow velocity (F_d , $\text{cm}^3 \text{cm}^{-2} \text{h}^{-1}$) was calculated according to the empirical calibration formula proposed by Granier (1987):

$$F_d = 0.0119 \left(\frac{\Delta T_{\max} - \Delta T}{\Delta T} \right)^{1.231} \times 3600 \quad (3)$$

Sapwood area (A_s , cm^2) thickness was derived from sapwood thickness investigations of the sample trees by using an increment borer and a vernier caliper at the end of the growing season. The mean sapwood areas of the sample trees from the ND, LD, and SD sites were 220.9, 114.4, and 95.9 cm^2 , respectively. The daily transpiration (Tr , mm d^{-1}) was calculated as follows:

$$Tr = (F_d \times A_s \times 24) / (A_c \times 10^3) \quad (4)$$

The Tr of each degradation class was the average value of five sample trees in the ND, LD, and SD sites, and the time series of the Tr of each sample tree is shown in Fig. A3 of Appendix A. Notably, the reason for not performing laboratory calibration on the TDP-20 was that several studies have found that laboratory calibration of sap flow for diffuse-porous species (i.e., *P. simonii*) is not significantly different from Granier's empirical calibration (Bush et al., 2010; Dai et al., 2020b; Taneda and Sperry, 2008). Uncertainties in the measurement of sap flow using TDP-20 are mainly from differences in sap flow radial transport velocity in the sapwood and differences in sap flow densities between different orientations of the same tree. These uncertainties in sap flow measurements may lead to uncertainty in transpiration estimation. Because we used the same standard sensor to measure the sap flow velocity of the same species and used the same methodology to estimate the daily transpiration, the uncertainties in measurement and transpiration estimation did not affect the comparison of water-use strategies in different plantations.

2.6. Leaf $\delta^{13}\text{C}$ and WUE_i

During photosynthesis in C₃ plants, photosynthetic carboxylases preferentially use ^{12}C to ^{13}C , and $^{13}\text{CO}_2$ diffuses more slowly than $^{12}\text{CO}_2$ through the stomata and boundary layer of leaf (Farquhar et al., 1982). Thus, leaf $\delta^{13}\text{C}$ is distinctly lower than that of CO₂ in air. Leaf $\delta^{13}\text{C}$ of C₃ plants is a reasonable proxy of WUE_i due to a significant positive correlation between them (Farquhar et al., 1989; Moreno-Gutiérrez et al., 2012). This method has been widely used for plant WUE_i estimation across various climates and species, and its advantage over instantaneous water-use efficiency is that it can reflect the long-term environmental adaptation of plants (Cernusak, 2018; Leffler and Evans, 2001; Wang et al., 2020; Wu et al., 2022; Zhao et al., 2021). The equation for calculating WUE_i according to Farquhar et al. (1982) is as follows:

$$\text{WUE}_i = \frac{\int A dt}{\int E dt} = \frac{c_a(1 - \phi)(b - \delta^{13}\text{C}_a + \delta^{13}\text{C})}{1.6\Delta e(b - a)} \quad (5)$$

where A and E are the rate of net photosynthesis and transpiration, respectively; c_a is the atmospheric CO₂ concentration; ϕ is the proportion of fixed carbon lost due to respiration in leaves and other plant tissues; Δe is the vapor pressure deficit between the intercellular spaces and external atmosphere; $\delta^{13}\text{C}_a$ and $\delta^{13}\text{C}$ are carbon isotope values for the atmosphere and plant leaves, respectively; a is the fractionation occurring due to diffusion in air (~4.4‰); b is the net fractionation caused by carboxylation (~27‰). Since the indicators of c_a, ϕ , Δe , and $\delta^{13}\text{C}_a$ were not measured in experimental plots, the WUE_i was not calculated directly in this study. Instead, the magnitude of WUE_i was indirectly estimated using leaf $\delta^{13}\text{C}$ values.

2.7. Statistical analysis

In this study, soil water at various depths was considered the water source for poplar trees. Because the groundwater level in the study area exceeded 40 m (Chen et al., 2008), the roots could not absorb and use groundwater; moreover, vegetation was not irrigated at the sampling sites. According to the SWC and soil water isotope values, we selected three soil layers in the 0–200 cm profile with significant differences ($P < 0.05$) in isotopic compositions as potential water sources: shallow (0–40 cm), middle (40–80 cm), and deep (80–200 cm) layers. The shallow layer had the most variability in soil water isotopes and SWC and was most susceptible to rainfall pulses and evaporation. The middle layer had relatively large variability in soil water isotopes and SWC and was vulnerable to heavy rainfall events. The deep layer had relatively stable variations in soil water isotopes and SWC and was poorly influenced by precipitation and evaporation. The relative contribution of each potential water source to the root water uptake of poplar trees was calculated using the MixSIR model with a Bayesian framework (Moore and Semmens, 2008). The MixSIR model can analyze multiple sources of water and incorporate the uncertainties of isotopic compositions and their fractionations in the establishment of posterior probability distributions of source water contributions. We assumed no isotopic fractionation during root water uptake (Dawson and Ehleringer, 1991) and set the fractionation coefficient to zero. We imported the source and mixture data ($\delta^2\text{H}$ and $\delta^{18}\text{O}$ in xylem water) into the model using MATLAB (2023a, MathWorks Inc., Natick, USA) and then set the iterations to one million times. The MATLAB software was obtained from a software library purchased by Northwest A&F University. The average relative contributions of each source to the posterior probability distributions were analyzed.

The differences in root weight density, isotopic compositions ($\delta^2\text{H}$, $\delta^{18}\text{O}$, and $\delta^{13}\text{C}$) of soil and plant, daily transpiration, and the proportion of root water uptake in the ND, LD, and SD plantations were analyzed using one-way ANOVA. The Tukey LSD method was used for post hoc multiple comparisons of variables. Statistical analyses were performed using SPSS 22 (IBM Inc., Chicago, USA).

3. Results

3.1. Horizontal and vertical root distributions

The horizontal root system of poplar trees was well-developed, and the average root weight densities at 200 cm from the trunk were 483.7, 399.9, and 235.1 g m⁻³ in the 0–200 cm soil profile in the ND, LD, and SD plantations, respectively. No significant difference ($P > 0.05$) in the average root weight density was found among the distances from the trunk (50, 100, and 200 cm) in the ND, LD, and SD plantations (Fig. 2). In the vertical root system, the root weight density decreased with increasing soil depth. The average root weight density in the 0–200 cm soil profile was 741.4, 559.8, and 446.3 g m⁻³ in the ND, LD, and SD plantations, respectively. The differences between these sites were significant ($P < 0.05$). As degradation intensified, the root proportion of the shallow layer gradually increased, and that of the middle and deep layers decreased. The root proportions of the shallow, middle, and deep layers were respectively 70.1%, 9.3%, and 20.6% in the ND plantations; 81.0%, 8.4%, and 10.6% in the LD plantations; and 91.2%, 6.0%, and 2.8% in the SD plantations.

3.2. Soil water status and transpiration

The cumulative precipitation was 230.9 mm from May to September. September had the lowest precipitation (Fig. 3a). The SWC of each potential water source (shallow, middle, and deep layers) for poplar trees is shown in Fig. 3b–d. The SWC of the shallow layer ranged from 0.019 to 0.066 cm³ cm⁻³ and responded rapidly to rainfall events. No significant difference ($P > 0.05$) in the mean SWC of the shallow layer was found among the ND, LD, and SD plantations (Fig. 3b). The SWCs of the middle and deep layers in the ND and LD plantations were not sensitive to rainfall events and showed a decreasing trend from May to September. We found significant differences ($P < 0.05$) in the average SWCs of the middle and deep layers among the ND, LD, and SD plantations (Fig. 3c, d). We also found that ND plantations had the lowest average SWCs in the middle and deep layers, and LD and SD plantations had the highest average SWCs in the middle and deep layers, respectively.

The Tr in the ND, LD, and SD plantations ranged from 0.04 to 2.38, 0.03–1.30, and 0.06–1.50 mm d⁻¹, respectively (Fig. 4). The average Tr in the ND, LD, and SD plantations were 0.93 ± 0.48 , 0.65 ± 0.27 , and 0.53 ± 0.26 mm d⁻¹, respectively, and the difference among them was significant ($P < 0.05$), indicating that plantation degradation reduced transpiration. From June to September, an overall trend of decreasing REW was observed for each site (Fig. 4b–d), which corresponded to the reduction in SWC for different soil layers (Fig. 3b–d). The Tr showed similar seasonal variation patterns among the experimental sites and varied synchronously with REW (e.g., Tr increased when REW increased) (Fig. 4b–d). The average Tr in the ND, LD, and SD plantations during the soil wet period (REW ≥ 0.4) were 1.34 ± 0.50 , 0.96 ± 0.26 , and 0.77 ± 0.27 mm d⁻¹, respectively, which were significantly ($P < 0.05$) higher than that during the soil dry period (REW < 0.4), with the values of 0.75 ± 0.48 , 0.56 ± 0.27 , and 0.43 ± 0.26 mm d⁻¹, respectively.

3.3. Isotopic compositions of different water pools

The $\delta^2\text{H}$ and $\delta^{18}\text{O}$ in precipitation varied from -151.78 to -6.99‰ and from -20.52 to -0.40‰ (Fig. 3a and Fig. 5a), and the precipitation-weighted averages (\pm standard deviation) were -48.65 ± 37.60 ‰ and -7.72 ± 5.17 ‰, respectively. The maximum and minimum monthly mean $\delta^2\text{H}$ and $\delta^{18}\text{O}$ in precipitation occurred in June and September, respectively. In the dual-isotope space (Fig. 5), the slope and intercept of the local meteoric water line (LMWL, $\delta^2\text{H} = 7.17\delta^{18}\text{O} + 3.19$, $R^2 = 0.97$) were smaller than those of the global meteoric water line (GMWL, $\delta^2\text{H} = 8\delta^{18}\text{O} + 10$) (Craig, 1961), reflecting the arid climate of the study area. With increasing depth, the data points of $\delta^2\text{H}$ - $\delta^{18}\text{O}$ in the soil water

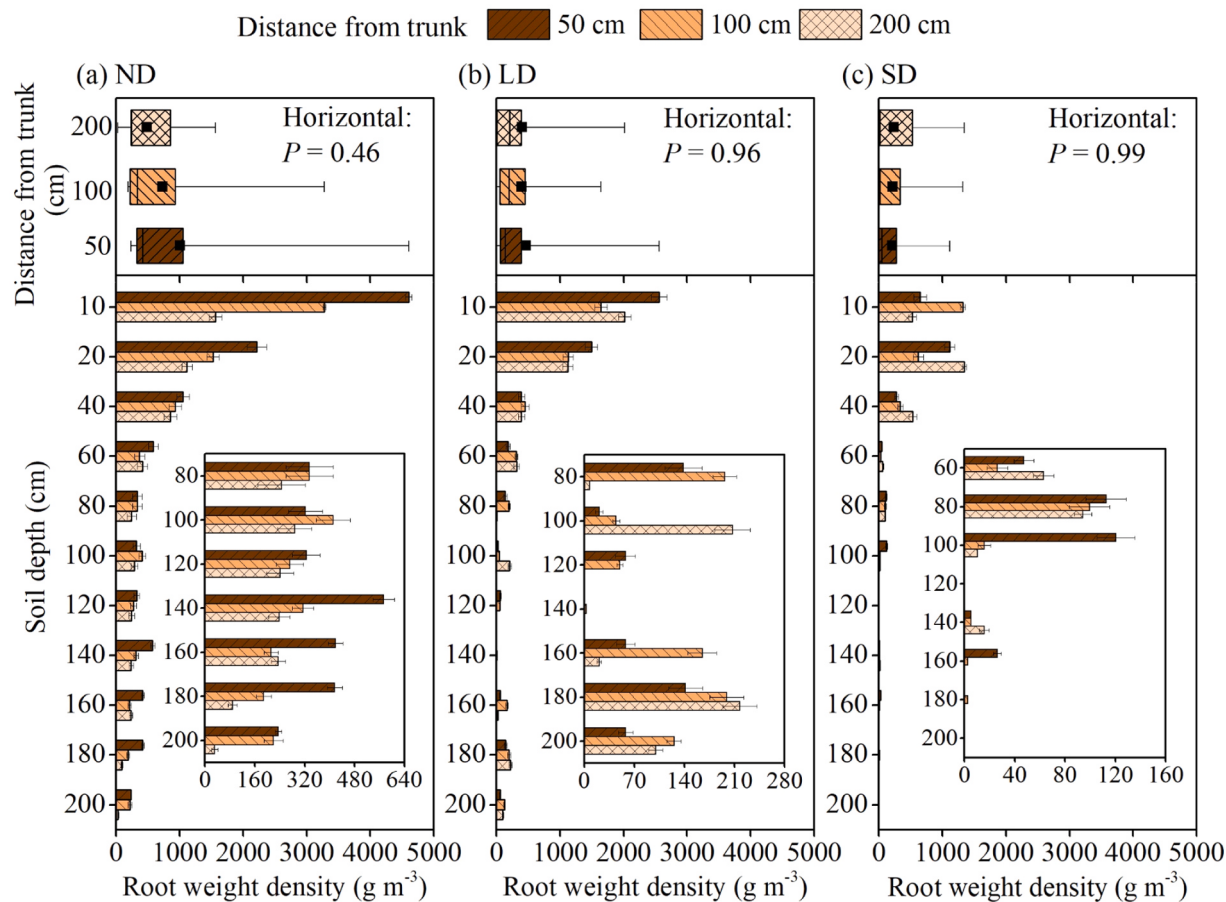


Fig. 2. Horizontal and vertical root distributions of poplar trees. Box plots show the minimum, 25%, median, 75%, and maximum root weight density at 50, 100, and 200 cm from the trunk in the 0–200 cm soil profile; black squares indicate the mean ($n=33$). The inset shows a properly enlarged vertical root distribution on the X-axis. Error bars show the standard deviation ($n=3$). ND, LD, and SD indicate no, lightly, and severely degraded plantations, respectively.

gradually approached and clustered toward the LMWL. The slope and intercept of the soil water line (SWL) in the ND plantations were similar to those in the LD plantations but were higher than those in the SD plantations (ND: $\delta^2\text{H}=4.298^{18}\text{O}-33.21$, $R^2=0.81$; LD: $\delta^2\text{H}=4.298^{18}\text{O}-34.59$, $R^2=0.87$; SD: $\delta^2\text{H}=4.058^{18}\text{O}-35.77$, $R^2=0.82$). The data points of $\delta^2\text{H}$ - $\delta^{18}\text{O}$ in the xylem water matched those in the soil water in the dual-isotope space (Fig. 5), implying no apparent deuterium depletion. We observed no significant differences ($P>0.05$) in the mean $\delta^2\text{H}$ and $\delta^{18}\text{O}$ in the soil and xylem waters among the ND, LD, and SD plantations (Table 2). Although seasonal variations in $\delta^2\text{H}$ and $\delta^{18}\text{O}$ in the shallow soil water were similar to those in precipitation (i.e., the maximum in June and the minimum in September), such distinct seasonal variations in $\delta^2\text{H}$ and $\delta^{18}\text{O}$ were not observed in the middle and deep soil water in the ND, LD, and SD plantations (Fig. 3 and Fig. 6). With increasing depth, soil water isotopes were gradually depleted in the ND, LD, and SD plantations (Fig. 6 and Table 2).

3.4. Water source apportionment

Similar seasonal variations in the main water absorption depths of poplar trees were observed in the ND, LD, and SD plantations (Fig. 7). Poplar trees in the ND and LD plantations mainly absorbed shallow soil water in May (the month when the soil was the wettest), with contributions of 63.1% and 61.7%, respectively, and poplar trees in the SD plantations mainly absorbed soil water at the depth of 40–80 cm (48.0%) in May (Fig. 7a, b). Poplar trees in the ND, LD, and SD plantations mainly absorbed soil water at the depth of 40–80 cm from June to August, with contribution proportions of 42.1–45.0%, 38.3–45.2%,

and 42.4–47.7%, respectively (Fig. 7a). Poplar trees in the ND, LD, and SD plantations mainly absorbed deep soil water in September (the month when the soil was the driest), with proportions of 45.9%, 51.6%, and 49.8%, respectively (Fig. 7a, b).

Based on the daily transpiration data of each site shown in Fig. 4, the absolute monthly consumption of soil water was calculated. From June to September, poplar trees in the ND, LD, and SD plantations consumed 14.3–38.1, 12.2–23.2, and 8.1–21.6 mm of soil water storage per month, respectively (Fig. 7c). Although the relative contribution proportion of deep soil water absorbed by poplar trees was the highest in September, the absolute use of the water source in this month was even lower than that in June or July (Fig. 7c). In other words, the high relative contribution proportion of deep soil water during severe soil drought conditions did not increase the absolute water use. Additionally, severe soil drought decreased the water use of the shallow and middle soil waters, and the combined effects resulted in extremely low transpiration in September.

3.5. Leaf $\delta^{13}\text{C}$ and WUE_i

The leaf $\delta^{13}\text{C}$ values of poplar trees in the ND, LD, and SD plantations ranged from $-27.54\text{\textperthousand}$ to $-26.93\text{\textperthousand}$, $-27.56\text{\textperthousand}$ to $-26.59\text{\textperthousand}$, and $-27.17\text{\textperthousand}$ to $-26.59\text{\textperthousand}$, respectively (Fig. 8a), and thus did not show significant seasonal variation ($P>0.05$). The mean leaf $\delta^{13}\text{C}$ values in the ND, LD, and SD plantations were $-27.2 \pm 0.2\text{\textperthousand}$, $-27.1 \pm 0.4\text{\textperthousand}$, and $-27.0 \pm 0.2\text{\textperthousand}$, respectively, and significant differences were not found among them ($P>0.05$). A weak positive correlation ($P>0.05$) was observed between leaf $\delta^{13}\text{C}$ and SWC in the ND plantations, and significant

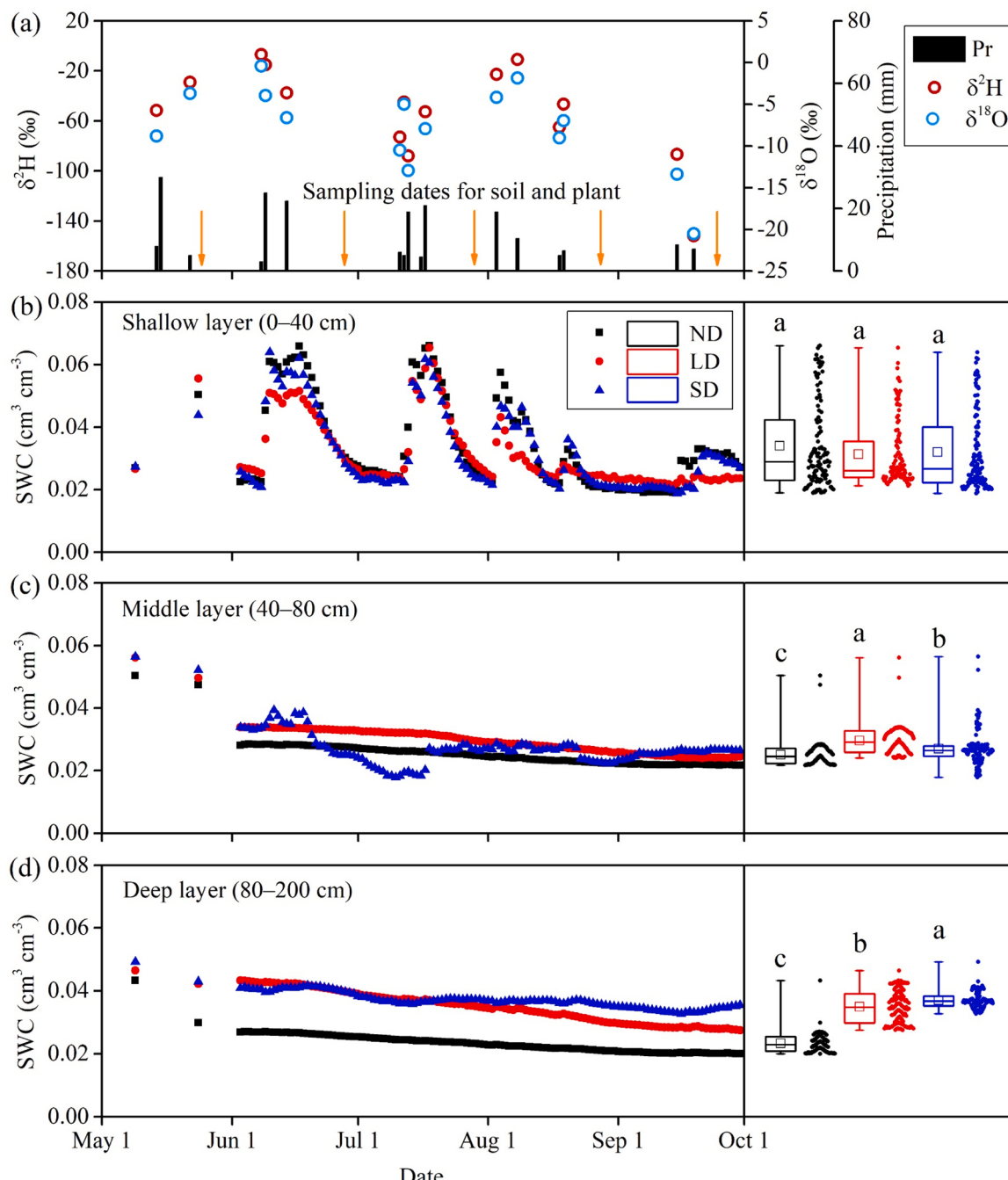


Fig. 3. Temporal variations in daily precipitation (Pr), $\delta^{2}\text{H}$ - $\delta^{18}\text{O}$ in precipitation (a), and soil water content (SWC) at various depths (b-d). The SWC in May is obtained from the soil gravimetric water content and soil bulk density. The box plots show the minimum, 25%, median, 75%, and maximum SWC; squares indicate the mean ($n=122$). Different lowercase letters in the box plots denote a significant difference in the mean SWC of the same soil layer among the sample sites ($P<0.05$). Orange arrows correspond to the sampling dates of soil and plant isotopes. ND, LD, and SD indicate no, lightly, and severely degraded plantations, respectively.

negative correlations ($P<0.05$) were observed between leaf $\delta^{13}\text{C}$ and SWC in the LD and SD plantations (Fig. 8b). The leaf $\delta^{13}\text{C}$ of C₃ plants is generally associated with the WUE_i, and a larger leaf $\delta^{13}\text{C}$ value corresponds to a higher WUE_i as illustrated in Eq. (5). The results showed that although plantation degradation did not directly affect WUE_i, it changed the sensitivity of WUE_i to soil water.

4. Discussion

4.1. Isotopic compositions of different water pools

Studies have shown that soil water isotopes are typically influenced by precipitation (Robertson and Gazis, 2006), evaporation (Lyu et al., 2021), and infiltration (Yang and Fu, 2017). Shallow soil water acquires most of the isotopic signals during precipitation and presents similar seasonal isotopic variations as precipitation. The slope of the SWL in the SD plantations was the lowest among the three sites, reflecting its strong soil evaporation (Lyu et al., 2021). Yang and Fu (2017) showed that

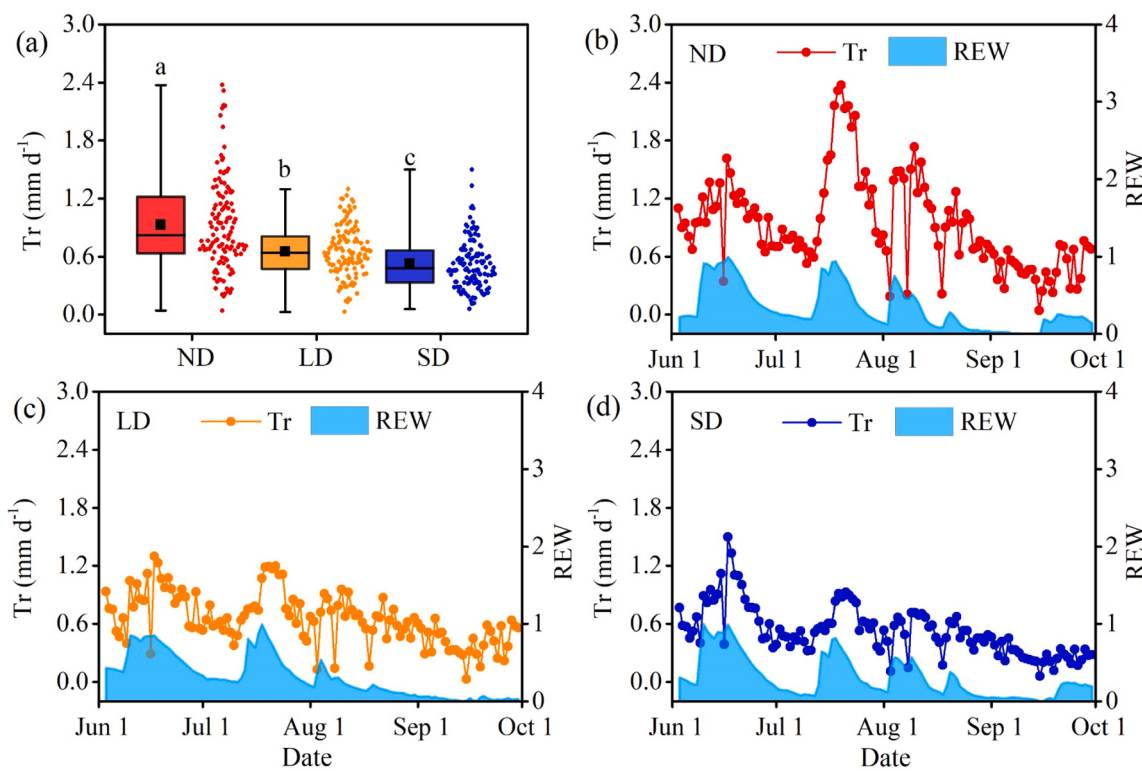


Fig. 4. Average daily transpiration (Tr) from June to September (a). Seasonal variation in transpiration and REW (b-d) at each site. Tr and REW represent transpiration and relative extractable water, respectively. Box plots show the minimum, 25%, median, 75%, and maximum transpiration; black squares indicate the mean ($n=120$). Different lowercase letters in the box plots denote a significant difference in average Tr among the sample sites ($P<0.05$). ND, LD, and SD indicate no, lightly, and severely degraded plantations, respectively.

when only one obvious peak soil water isotope value (close to that of previous precipitation) appeared in the vertical profile, precipitation infiltrated unsaturated soil in the form of piston flow. However, when more than one peak soil water isotope value appeared in the vertical profile, an increase in SWC occurred that may indicate preferential flow. The results of the aforementioned method demonstrated that precipitation infiltration occurred in the form of piston flow in the ND, LD, and SD plantations (Fig. 3 and Fig. 6). In summary, we inferred that similar precipitation infiltration and hydraulic redistribution in the ND, LD, and SD plantations might result in the stability of soil water isotopes. However, Liu et al. (2020) reported differences in soil water isotopes in poplar plantations under different degrees of degradation, which could be attributed to changes in the soil physical properties and groundwater recharge.

Although poplar trees in the ND plantations showed a relatively abundant and deep root system (Fig. 2) and may prefer to use deep soil water (relatively depleted in heavy isotopes), resulting in depleted isotopes in its xylem water, the low soil water availability in the deep layer (Fig. 3) limited the water uptake from deep soils. However, poplar trees in the degraded plantations had a relatively sparse and shallow root system (Fig. 2) and absorbed a certain amount of water from the deep layer owing to high soil water availability (Fig. 3). Therefore, the water source apportionment of poplar trees may have been consistent across the sites. The xylem water isotopes of poplar trees were consistent with the soil water isotopes (Fig. 5), indicating no obvious isotopic fractionation during root water uptake and water transport. That is a prerequisite for determining the water source apportionment based on the stable isotope method. This result was inconsistent with that of Zhao and Wang (2021) for *Salix matsudana* at a check-dammed channel in the catchment; they suggested that isotopic fractionation might be related to the soil water conditions (Zhao et al., 2022).

Uncertainty in the extraction methodology of xylem and soil water

may affect isotope analysis results and the calculation of the contribution proportion of soil water to xylem water at different depths. The cryogenic vacuum distillation (CVD) method is widely used to extract water from soil and plant xylem for isotope analyses (Orłowski et al., 2018). On the basis of observations of a significant ²H fractionation, investigations have begun to question the interpretation of plant water isotopes obtained using CVD. Chen et al. (2020) conducted a rehydration experiment and suggested that the xylem water cryogenic extraction error is from a dynamic exchange between organically bound deuterium and liquid water during water extraction. However, Diao et al. (2022) observed that ²H fractionation had an inversely proportional relationship with the absolute amount of water being extracted and that the methodological uncertainties can be controlled when sufficiently high amounts of xylem water were extracted (>0.6 mL). In our study, all xylem water samples obtained through CVD were approximately 1.0 mL, and the isotope fractionation during CVD extraction of water was negligible. Owing to evidence showing that cryogenically extracted soil water is depleted relative to reference water, some researchers have also questioned CVD's accuracy in extracting soil water. Wen et al. (2021) and Yang et al. (2023) have found that cryogenic extraction biases were positively correlated with soil clay content. Orłowski et al. (2018) demonstrated that sandy soil was almost unaffected by cryogenic extraction biases. In our study, the soil texture at each site was sandy, and the granular composition was 95.7% sand, 3.2% silt, and 1.1% clay. Moreover, no isotopic offset between soil water and xylem water was found based on Fig. 5. Thus, the methodological uncertainty in the extraction of xylem and soil water by CVD is probably negligible in this study.

4.2. Water-use strategy

As summarized in Fig. 9, transpiration significantly decreased as

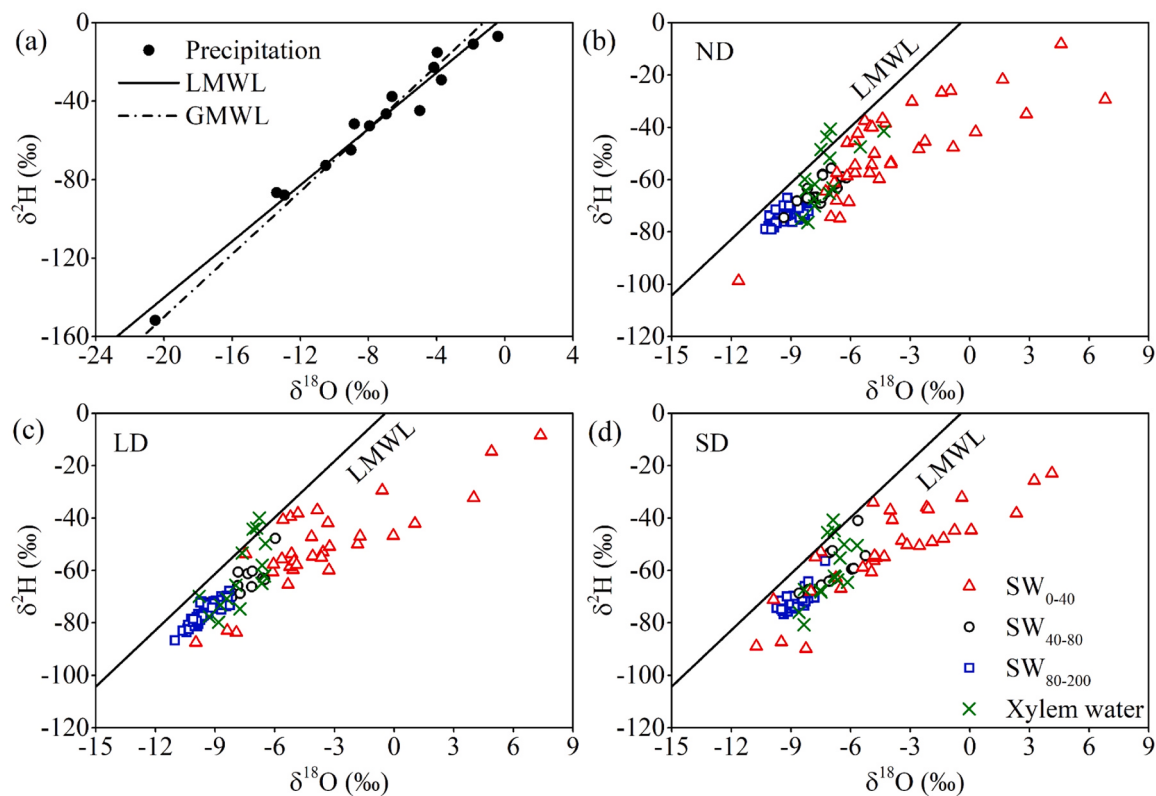


Fig. 5. Relationships between $\delta^2\text{H}$ and $\delta^{18}\text{O}$ in precipitation (a), soil water, and xylem water in different plantations (b–d). LMWL represents the local meteoric water line ($\delta^2\text{H}=7.17\delta^{18}\text{O}+3.19$, $R^2=0.97$, $n=15$); GMWL represents the global meteoric water line ($\delta^2\text{H}=8\delta^{18}\text{O}+10$). SW₀₋₄₀, SW₄₀₋₈₀, and SW₈₀₋₂₀₀ represent the soil water in shallow (0–40 cm), middle (40–80 cm), and deep (80–200 cm) layers, respectively. ND, LD, and SD indicate no, lightly, and severely degraded plantations, respectively.

Table 2

Mean $\delta^2\text{H}$ and $\delta^{18}\text{O}$ in the soil and xylem water of poplar trees during the growth season.

Sampling site	Shallow soil water	Middle soil water	Deep soil water	Xylem water
$\delta^2\text{H}$ (%)	ND -48.71 ± 17.32	-64.09 ± 4.94	-73.88 ± 3.12	-58.43 ± 12.00
	LD -50.11 ± 18.43	-65.53 ± 6.89	-75.90 ± 4.14	-61.85 ± 13.02
	SD -52.54 ± 18.43	-59.65 ± 8.15	-72.32 ± 3.16	-59.97 ± 11.75
$\delta^{18}\text{O}$ (%)	ND -3.89 ± 3.62	-7.53 ± 0.82	-9.18 ± 0.62	-7.28 ± 1.11
	LD -3.76 ± 4.11	-7.66 ± 0.94	-9.45 ± 0.65	-7.70 ± 1.10
	SD -4.05 ± 3.64	-6.86 ± 1.03	-8.85 ± 0.49	-7.07 ± 0.85

Values are shown as the mean \pm standard deviation ($n=5$). ND, LD, and SD indicate no, lightly, and severely degraded plantations, respectively. No significant difference ($P>0.05$) in the mean $\delta^2\text{H}$ and $\delta^{18}\text{O}$ values of shallow soil water, middle soil water, deep soil water, and xylem water, across the ND, LD, and SD plantations.

plantation degradation intensified ($P<0.05$). Moreover, the higher the degradation degree, the lower the DBH, crown width, and root biomass of the tree (Fig. 1, Fig. 2, and Fig. 9), and the less water necessary for plantation growth. Reduced water demand of degraded plantations facilitated deep soil water storage (Fig. 3 and Fig. 9). These findings support our hypothesis (1). However, hypothesis (2) that degraded plantations reduce the relative contribution and absolute use of deep soil water was partly rejected. According to the MixSIR model, poplar trees shifted their water source from shallow to deep layers in the process of soil wetting to drying (Fig. 7a, b). The same results were found for *Pinus tabuliformis* and *Hippophae rhamnoides* in semi-arid regions (Tang et al., 2018). The root water uptake patterns were similar in time and depth in

the ND, LD, and SD plantations (Fig. 7a and Fig. 9), indicating that the ability of trees in degraded plantations to absorb deep soil water did not change. These findings are inconsistent with those of Liu et al. (2020) and Liu et al. (2021). In these studies, as degradation intensified, poplar trees gradually lost their ability to obtain water from deep soil, which was related to the small tree size and shallow root distribution. However, in our study, the undiminished plasticity in deep soil water absorption of degraded plantations might be associated with a small number of roots still distributed in the deep layer (Fig. 2c and Fig. 9). Furthermore, a potential water source for tree utilization was provided by the deep layer because of the high SWC (Fig. 3d and Fig. 9).

Surprisingly, during the severe water stress in September, deep soil contributed the largest proportion of water for transpiration but did not compensate for the low water availability of the shallow and middle layers (Fig. 7), which was consistent with the findings of Gessler et al. (2022). These researchers found that beech did not have a compensating mechanism for deep roots during water stress and that water use depended mainly on water availability in the upper soil. We accepted the explanation that deep roots become impotent because soil drought severely inhibits underground metabolism, carbon allocation to roots, and root growth (Joseph et al., 2020). In addition, this effect might also be related to the depletion of available water in the deep layer. In the late growing season, the nearly exhausted deep soil water compensates little for the shortage of shallow soil water (Fig. 3). Therefore, the increased relative contribution proportion of deep soil water use during drought should be considered along with the absolute consumption of deep water because plantations might suffer degradation when deep soil water is insufficient to support normal growth.

Zhao and Wang (2021) suggested that leaf $\delta^{13}\text{C}$ is related to photorespiration, carbon isotopic fractionation after photosynthesis, and changes in environmental conditions. The variations in environmental

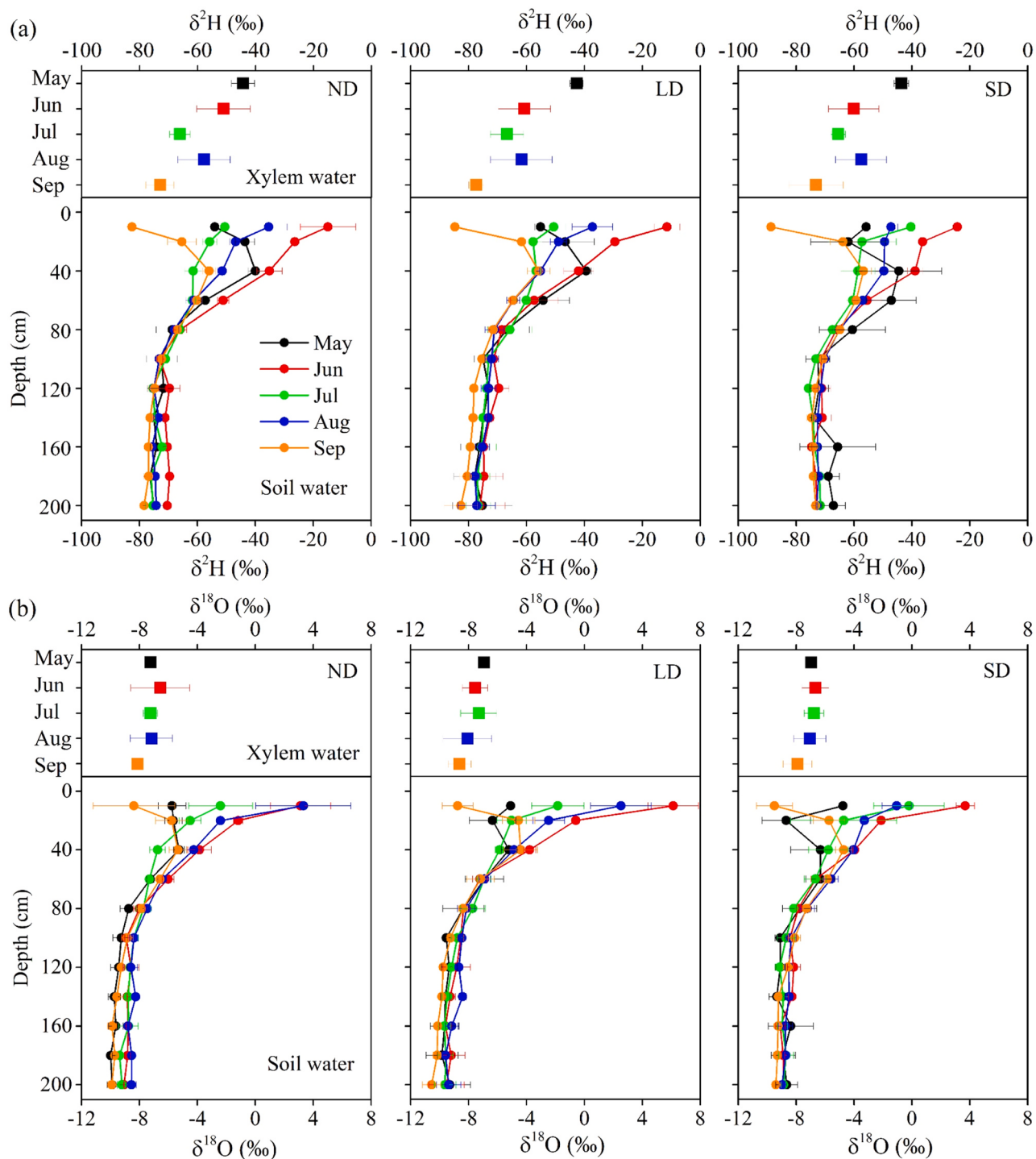


Fig. 6. Seasonal variations in $\delta^2\text{H}$ (a) and $\delta^{18}\text{O}$ (b) in the soil and xylem water. Values are shown as the mean \pm standard deviation ($n=3$). ND, LD, and SD indicate no, lightly, and severely degraded plantations, respectively.

conditions (temperature, humidity, and atmospheric carbon dioxide concentration) in the ND, LD, and SD plantations were the same, as was the variation in carbon assimilation and transpiration in the same species, which might have resulted in the consistency among leaf $\delta^{13}\text{C}$ and WUE_i (Fig. 8a). Notably, the relationships between leaf $\delta^{13}\text{C}$ of poplar trees and SWC were inconsistent in the ND, LD, or SD plantations (Fig. 8b). Leaf $\delta^{13}\text{C}$ in the ND plantations showed a weak positive correlation with SWC, which was similar to the results of Wang et al. (2020). Leaf $\delta^{13}\text{C}$ in the LD and SD plantations showed a negative correlation with SWC (Fig. 8b and Fig. 9), consistent with the results of Ale

et al. (2018). With decreasing soil water availability, the reduced stomatal conductance of poplar trees often resulted in a decrease in the ratio of intercellular to atmospheric partial pressure of CO_2 , and then the leaf $\delta^{13}\text{C}$ and WUE_i increased (Prentice et al., 2011). These findings suggest that poplar trees in degraded plantations could enhance their drought adaptability by improving WUE_i under soil water stress.

4.3. Implications for water management in afforestation ecosystems

Populus simonii is a fast-growing tree with high canopy transpiration

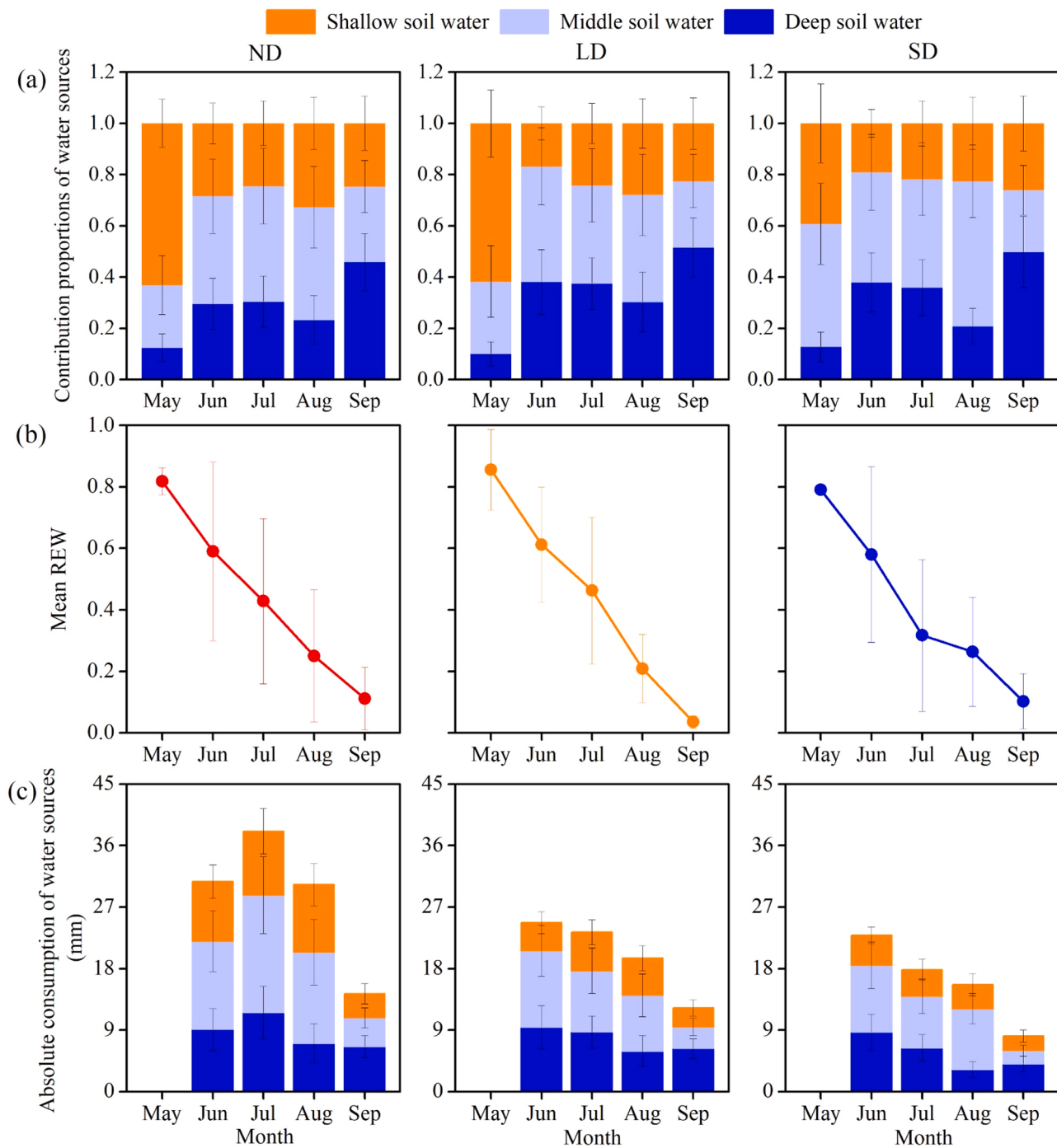


Fig. 7. Seasonal variations in the contribution proportions of water sources (a), mean REW (relative extractable water) (b), and absolute consumption of water sources (c) to poplar trees water absorption. Absolute water consumption is the product of source water contribution proportions and monthly cumulative transpiration of poplar trees. Values are shown as the mean \pm standard deviation. ND, LD, and SD indicate no, lightly, and severely degraded plantations, respectively.

demands (Wang et al., 2019) and survival ability (Sun et al., 2018), and in the 1990 s, it represented the local vanguard tree species for afforestation and restoration in this study area. However, since then, deep soil desiccation has been observed, and vegetation afforestation in semi-arid areas has been implicated (Zhang et al., 2018). When the water source in the upper soil is insufficient to fulfill the demand for plantation growth, the water use in the deep layer increases, and with long-term insufficient amounts of precipitation in water-limited areas, soil desiccation occurs. Additionally, studies have been reporting plantation degradation (Chen et al., 2015; Liu et al., 2020; Sun et al., 2018), and the attention to the link between plantation degradation and soil

water status has been increasing (Liang et al., 2022; Liu et al., 2020). In this study, due to the large transpiration and developed root system in the ND plantations, the SWCs in the middle and deep layers were significantly lower than those in the LD and SD plantations during the growing period (Fig. 2, Fig. 3, and Fig. 9). Moreover, precipitation could not easily infiltrate into the middle and deep layers in this study area (Fig. 3), hindering the replenishment of deep soil water. In the long term, limited soil water conditions hinder plantation growth. According to McDowell et al. (2008), under prolonged water stress, trees might suffer from carbon starvation and a cascade of downstream effects caused by the avoidance of drought-induced hydraulic failure via

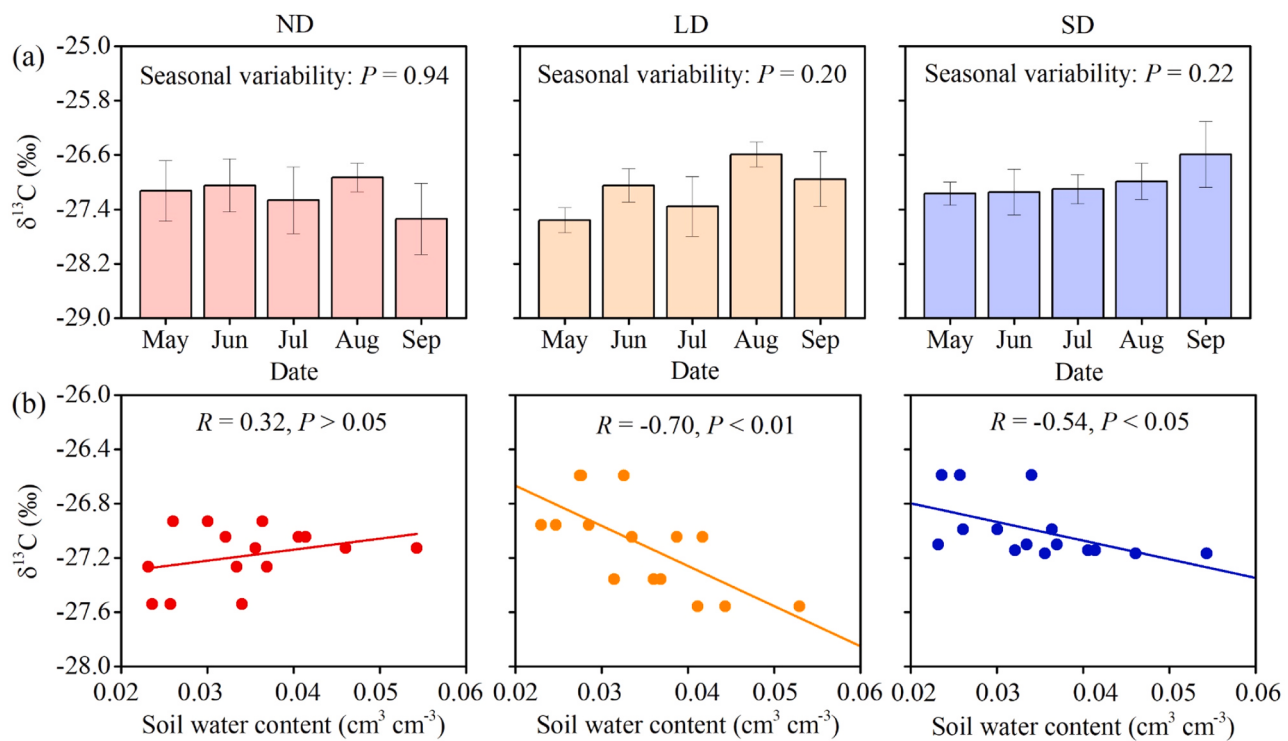


Fig. 8. Seasonal variations in the average leaf $\delta^{13}\text{C}$ (\pm standard deviation, $n=3$) of poplar trees (a) and their relationship with soil water content (b). Soil water content is the monthly average SWCs in the shallow (0–40 cm), middle (40–80 cm), and deep (80–200 cm) layers. ND, LD, and SD indicate no, lightly, and severely degraded plantations, respectively.

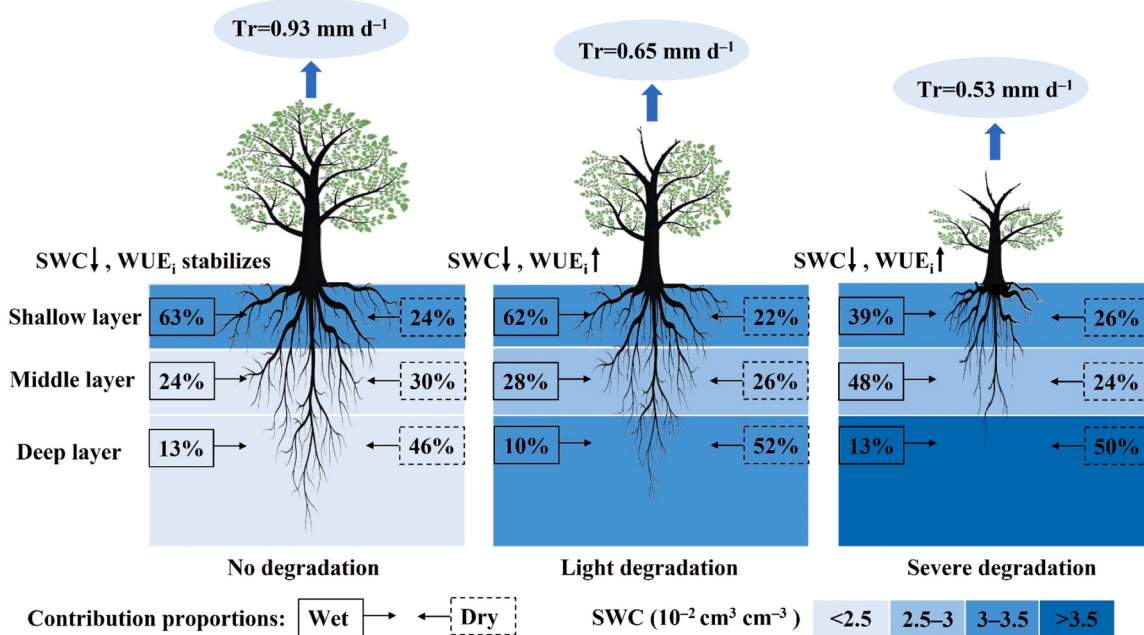


Fig. 9. Graphical summary of tree morphological characteristics, soil water status, and water-use strategies under different degradation degrees during the growing period. The soil water content (SWC) and transpiration (Tr) in the figure represent the mean values for each site during the growing period. Data in the solid and dashed boxes represent the average proportion of soil water use in May (the wettest month) and September (the driest month), respectively. As the SWC decreases, the intrinsic water-use efficiency (WUE_i) in the no degraded plantations stabilizes, and the WUE_i in the lightly degraded and severely degraded plantations tends to increase.

stomatal closure. In addition, poplar trees in the ND plantations showed greater height, DBH, and canopy and tended to carry a higher risk of hydraulic failure than in the LD and SD plantations (Bennett et al., 2015).

Water shortage is the main problem of poplar plantations in the study area. Although rational irrigation measures are essential to maintain the sustainable development of plantations in water-limited areas (Liu et al., 2022; Xi et al., 2021; Yamani et al., 2018), most of the plantations in the

semi-arid zone of the Loess Plateau are rain-fed. Due to the deep groundwater table (>40 m), complex topographic conditions, and underdeveloped irrigation systems in the study area, it is difficult for local farmers to use groundwater for large-scale irrigation of poplar plantations. In our study, the total precipitation for June–September 2021 is 186.4 mm (Fig. 3) and the estimated transpiration for ND, LD, and SD plantations is 113.0, 79.2, and 64.0 mm, respectively (Fig. 7). The high potential evapotranspiration (Wang et al., 2019) and sandy soils ($>95\%$ sand content) may result in high soil evaporation. Additionally, canopy interception evaporation also has a substantial water consumption in poplar plantations. Thus, in the rain-fed plantations, we should consider reducing unproductive water consumption (i.e. soil evaporation and canopy interception) and reducing excessive stand water consumption to maintain the sustainability of plantations. The bearing capacity of vegetation in relation to soil water and forest thinning should be considered to ensure that precipitation matches plantation growth and gradually replenishes the deep soil water. For no degraded plantations, we can remove some trees, trim the lower canopy side branches to reduce the canopy density, and cover the ground with these branches, to increase net precipitation and reduce soil evaporation. For degraded plantations, the main management measure is to cover the ground with pruned branches and leaves from no degraded plantations to reduce the high soil evaporation caused by the low canopy density, accelerating the recovery of soil water status. Additionally, a mixed tree-shrub pattern should be considered to increase biodiversity. Hydrological niche separation between species in mixed forests can improve resource allocation (Moreno-Gutiérrez et al., 2012) and alleviate water depletion in deep soils to a certain extent (Wang et al., 2020; Dai et al., 2023a).

5. Conclusion

In this study, we found similar seasonal isotopic patterns and isotopic profile distributions of the soil water and xylem water in the three plantations. As plantation degradation intensified, the root biomass decreased and the root proportion of the deep layer decreased. Although differences were not observed in the SWC of the shallow layer among the ND, LD, and SD plantations, the SWCs of the middle and deep layers in the ND plantations were lower than those in the LD and SD plantations. Compared with no degraded plantations, degraded plantations reduced

transpiration but did not change root water uptake patterns. Poplar trees under different degradation classes shifted the water source from shallow to deep layers in the process of soil wetting to drying. Thus, our findings supported hypothesis (1) that the deep roots and transpiration decrease with increased degradation. However, hypothesis (2) that degraded plantations reduce the relative contribution and absolute use of deep soil water was partly rejected. Additionally, the sensitivity of WUE_i to SWC for degraded plantations increased compared with that of no degraded plantations. In conclusion, the normal growth of poplar plantations is prone to soil desiccation of deep layers to high transpiration demand; degraded poplar plantations alleviate water depletion of deep soils due to low transpiration demand. For rainfed poplar plantations in water-limited areas, proper thinning and measures of reducing soil evaporation may be necessary.

CRediT authorship contribution statement

Junjie Dai: Writing – original draft, Visualization, Software, Investigation, Formal analysis, Data curation, Conceptualization. **Ying Zhao:** Writing – review & editing, Visualization, Validation, Methodology, Investigation. **Katsutoshi Seki:** Writing – review & editing, Validation, Software. **Li Wang:** Writing – review & editing, Visualization, Supervision, Resources, Project administration, Funding acquisition.

Declaration of Competing Interest

The authors declare that they have no known competing financial interests or personal relationships that could have appeared to influence the work reported in this paper.

Data availability

Data will be made available on request.

Acknowledgements

This work was supported by the National Natural Science Foundation of China (grant numbers 42171043 and 42377318).

Appendix A

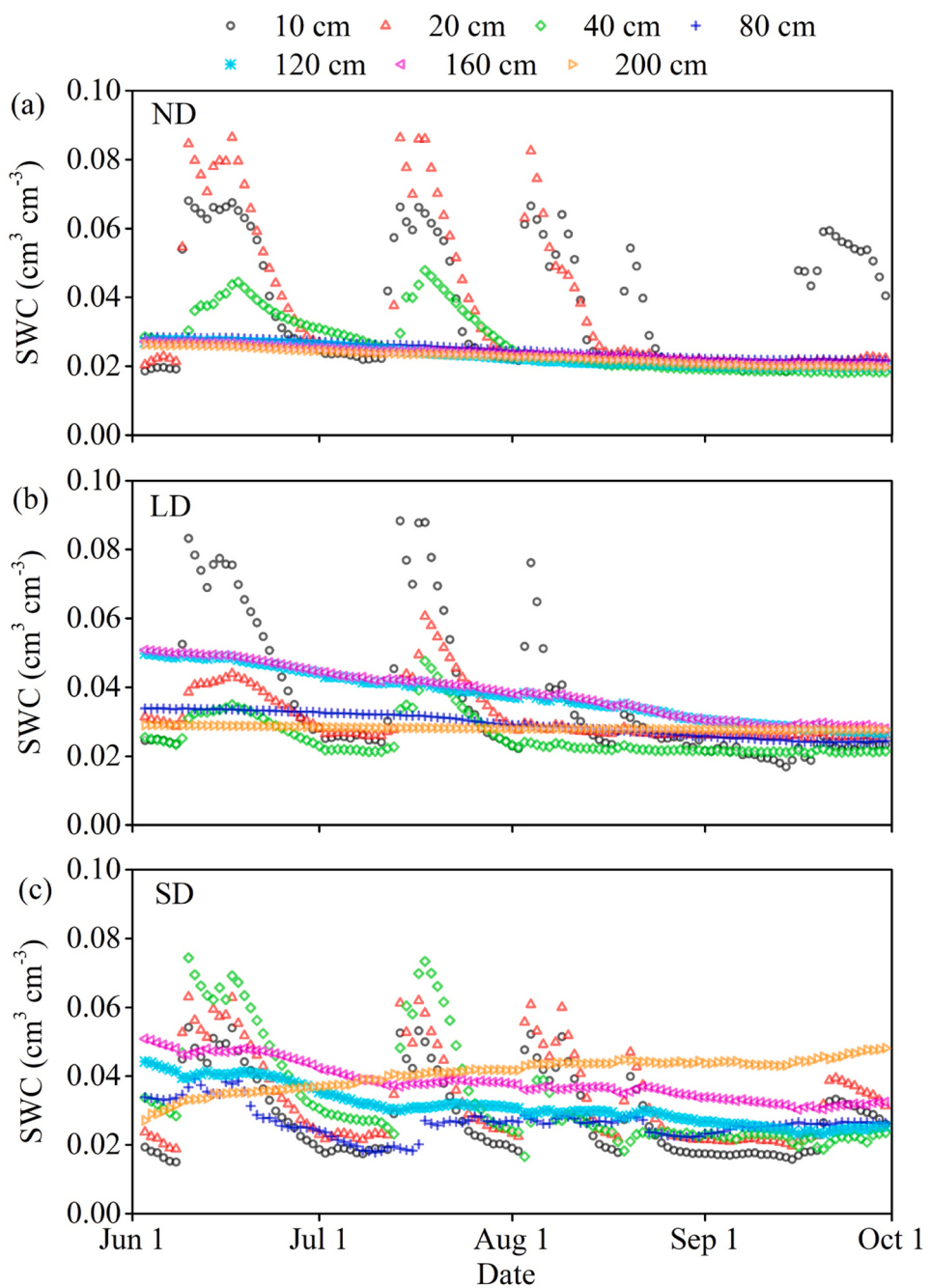


Fig. A1. Daily variation in soil volumetric water content (SWC) at different depths for each degradation class monitored by sensors from June to September. ND, LD, and SD indicate no, lightly, and severely degraded plantations, respectively.

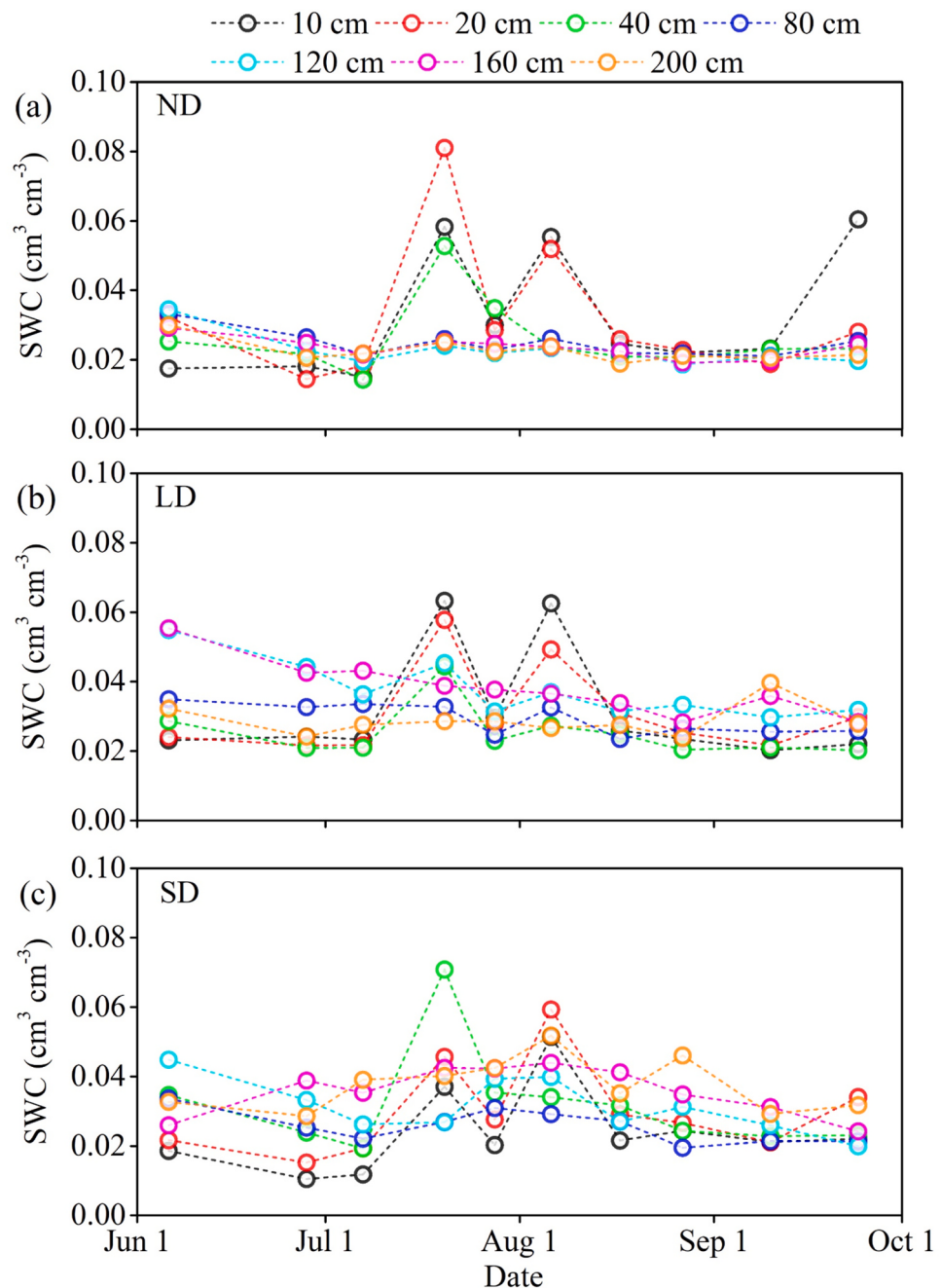


Fig. A2. Daily variation in soil volumetric water content (SWC) at different depths for each degradation class monitored by manual measurement (soil gravimetric water content times soil bulk density) from June to September.

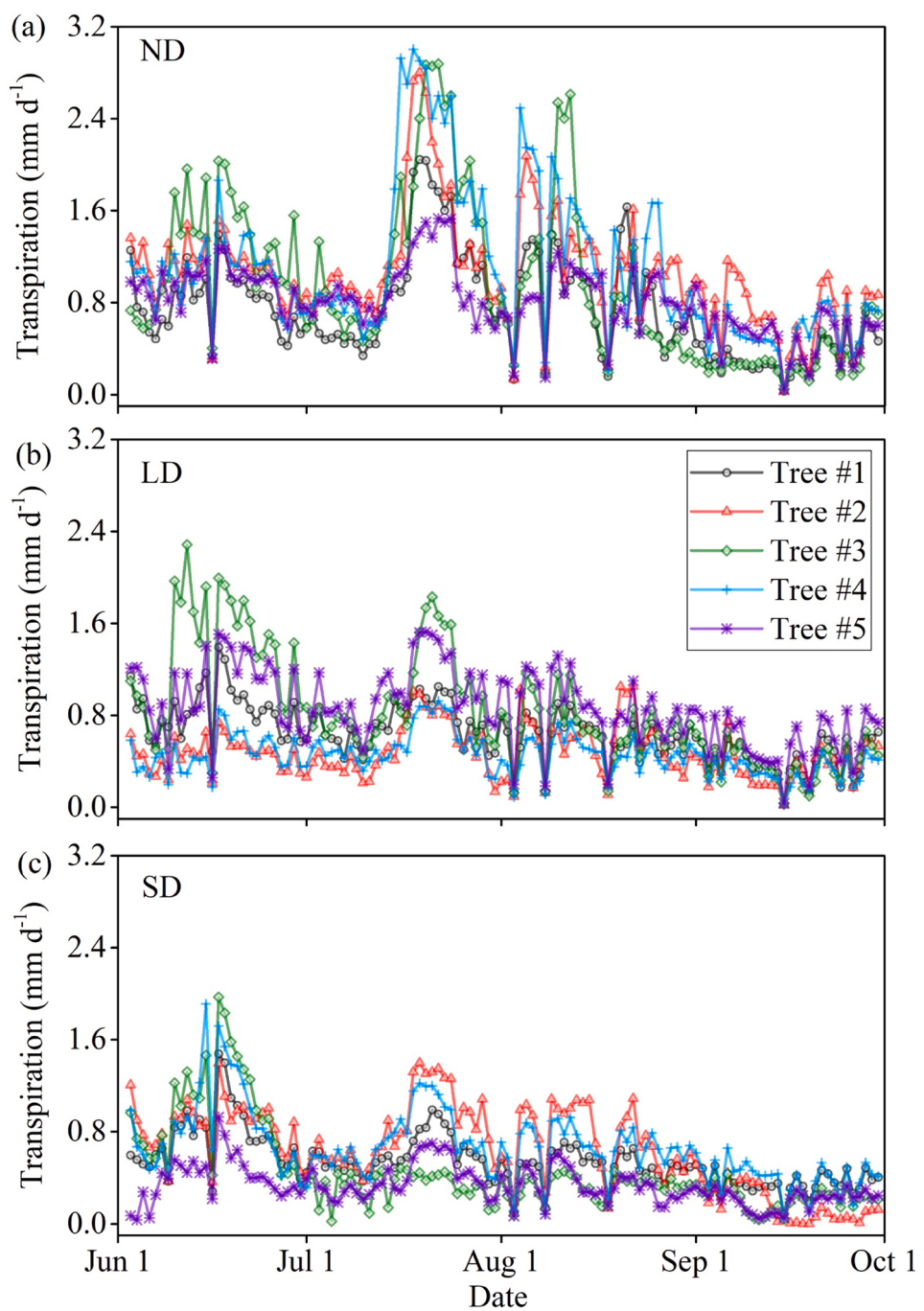


Fig. A3. Daily variation in transpiration in five sample trees of each degradation class from June to September.

References

- Ale, R., Zhang, L., Li, X., Raskoti, B.B., Pugnaire, F.I., Luo, T., 2018. Leaf $\delta^{13}\text{C}$ as an indicator of water availability along elevation gradients in the dry Himalayas. *Eco. Indic.* 94, 266–273.
- Allen, C.D., Macalady, A.K., Chenchouni, H., Bachelet, D., McDowell, N., Vennetier, M., Kitzberger, T., Rigling, A., Breshears, D.D., Hogg, E.H., et al., 2010. A global overview of drought and heat-induced tree mortality reveals emerging climate change risks for forests. *Ecol. Manag.* 259, 660–684.
- Bennett, A.C., McDowell, N.G., Allen, C.D., Anderson-Teixeira, K.J., 2015. Larger trees suffer most during drought in forests worldwide. *Nat. Plants* 1, 1–5.
- Brinkmann, N., Eugster, W., Zweifel, R., Buchmann, N., Kahmen, A., 2016. Temperate tree species show identical response in tree water deficit but different sensitivities in sap flow to summer soil drying. *Tree Physiol.* 36, 1508–1519.
- Bush, S.E., Hultine, K.R., Sperry, J.S., Ehleringer, J.R., 2010. Calibration of thermal dissipation sap flow probes for ring- and diffuse-porous trees. *Tree Physiol.* 30, 1545–1554.
- Cernusak, L.A., 2018. Gas exchange and water-use efficiency in plant canopies. *Plant Biol.* 22, 52–67.
- Chen, C., Park, T., Wang, X., Piao, S., Xu, B., Chaturvedi, R.K., Fuchs, R., Brovkin, V., Clais, P., Fensholt, R., et al., 2019. China and India lead in greening of the world through land-use management. *Nat. Sustain.* 2, 122–129.
- Chen, H., Shao, M., Li, Y., 2008. Soil desiccation in the Loess Plateau of China. *Geoderma* 143, 91–100.
- Chen, Y., Wang, K., Lin, Y., Shi, W., Song, Y., He, X., 2015. Balancing green and grain trade. *Nat. Geosci.* 8, 739–741.
- Chen, Y., Helliker, B.R., Tang, X., Li, F., Zhou, Y., Song, X., 2020. Stem water cryogenic extraction biases estimation in deuterium isotope composition of plant source water. *P. Natl. Acad. Sci. USA* 118, 33345–33350.

- Choat, B., Brodribb, T.J., Brodersen, C.R., Duursma, R.A., López, R., Medlyn, B.E., 2018. Triggers of tree mortality under drought. *Nature* 558, 531–539.
- Craig, H., 1961. Isotopic variations in meteoric water. *Science* 133, 1702–1703.
- Dai, J., Zhang, X., Luo, Z., Wang, R., Liu, Z., He, X., Rao, Z., Guan, H., 2020a. Variation of the stable isotopes of water in the soil-plant-atmosphere continuum of a *Cinnamomum camphora* woodland in the East Asian monsoon region. *J. Hydrol.* 589, 125199.
- Dai, J., Zhang, X., Wang, L., Luo, Z., Wang, R., Liu, Z., He, X., Rao, Z., Guan, H., 2022. Seasonal isotopic cycles used to identify transit times and the young water fraction within the critical zone in a subtropical catchment in China. *J. Hydrol.* 612, 128138.
- Dai, J., Li, Y., Wang, L., 2023a. Mixed-species plantations alleviate deep soil water depletion and facilitate hydrological niche partitioning compared to pure plantations. *Ecol. Manag.* 539, 121017.
- Dai, J., Zhao, Y., Wang, L., 2023b. Characteristic and modeling of sap flow of degraded *Populus simonii* in areas where the ecology is vulnerable. *Land Degrad. Dev.* 34, 493–505.
- Dai, J., Zhang, X., Wang, L., Wang, R., Luo, Z., He, X., Rao, Z., 2023c. Water stable isotope characteristics and water use strategies of co-occurring plants in ecological and economic forests in subtropical monsoon regions. *J. Hydrol.* 621, 129565.
- Dai, Y., Wang, L., Wan, X., 2020b. Frost fatigue and its spring recovery of xylem conduits in ring-porous, diffuse-porous, and coniferous species in situ. *Plant Physiol. Bioch.* 146, 177–186.
- Dawson, T.E., Ehleringer, J.R., 1991. Streamside trees that do not use stream water. *Nature* 350, 335–337.
- Diao, H., Schuler, P., Goldsmith, G.R., Siegwolf, R.T.W., Saurer, M., Lehmann, M.M., 2022. Technical note: on uncertainties in plant water isotopic composition following extraction by cryogenic vacuum distillation. *Hydrolog. Earth Syst. Sci.* 26, 5835–5847.
- Ding, Y., Nie, Y., Chen, H., Wang, K., Querejeta, J.I., 2021. Water uptake depth is coordinated with leaf water potential, water-use efficiency and drought vulnerability in karst vegetation. *N. Phytol.* 229, 1339–1353.
- Farquhar, G.D., O'Leary, M.H., Berry, J.A., 1982. On the relationship between carbon isotope discrimination and the intercellular carbon dioxide concentration in leaves. *Func. Plant Biol.* 9, 121–137.
- Farquhar, G.D., Ehleringer, J.R., Hubick, K.T., 1989. Carbon isotope discrimination and photosynthesis. *Annu. Rev. Plant Biol.* 40, 503–537.
- Gessler, A., Bächli, L., Freund, E.R., Treydte, K., Schaub, M., Haeni, M., Weiler, M., Seeger, S., Marshall, J., Hug, C., et al., 2022. Drought reduces water uptake in beech from the drying topsoil, but no compensatory uptake occurs from deeper soil layers. *N. Phytol.* 233, 194–206.
- Grainer, A., 1987. Evaluation of transpiration in a Douglas-fir stand by means of sap flow measurements. *Tree Physiol.* 3, 309–320.
- Grossiord, C., Gessler, A., Grainer, A., Berger, S., Bréchet, C., Hentschel, R., Homme, R., Scherer-Lorenzen, M., Bonal, D., 2014. Impact of interspecific interactions on the soil water uptake depth in a young temperate mixed species plantation. *J. Hydrol.* 519, 3511–3519.
- Guo, Z., 2021. Soil water carrying capacity for vegetation. *Land Degrad. Dev.* 32, 3801–3811.
- Iqbal, S., Zha, T., Jia, X., Hayat, M., Qian, D., Bourque, C.P., Tian, Y., Bai, Y., Liu, P., Yang, R., et al., 2021. Interannual variation in sap flow response in three xeric shrub species to periodic drought. *Agr. Meteorol.* 297, 108276.
- Jia, X., Shao, M., Zhu, Y., Luo, Y., 2017. Soil moisture decline due to afforestation across the Loess Plateau, China. *J. Hydrol.* 546, 113–122.
- Joseph, J., Gao, D., Backes, B., Bloch, C., Brunner, I., Gleixner, G., Haeni, M., Hartmann, H., Hoch, G., Hug, C., et al., 2020. Rhizosphere activity in an old-growth forest reacts rapidly to changes in soil moisture and shapes whole-tree carbon allocation. *Proc. Natl. Acad. Sci. USA* 117, 24885–24892.
- Leffler, A.J., Evans, A.S., 2001. Physiological variation among *Populus fremontii* populations: short- and long-term relationships between $\delta^{13}\text{C}$ and water availability. *Tree Physiol.* 21, 1149–1155.
- Liang, X., Xin, Z., Shen, H., Yan, T., 2022. Deep soil water deficit causes *Populus simonii* Carr degradation in the three north shelterbelt region of China. *J. Hydrol.* 612, 128201.
- Liu, J., Li, D., Fernández, J., Coleman, M., Hu, W., Di, N., Zou, S., Liu, Y., Xi, B., Clothier, B., 2022. Variations in water-balance components and carbon stocks in poplar plantations with differing water inputs over a whole rotation: implications for sustainable forest management under climate change. *Agr. Meteorol.* 320, 108958.
- Liu, Z., Jia, G., Yu, X., 2020. Variation of water uptake in degradation agroforestry shelterbelts on the North China Plain. *Agr. Ecosyst. Environ.* 287, 106697.
- Liu, Z., Jia, G., Yu, X., Lu, W., Sun, L., Wang, Y., Zierdie, B., 2021. Morphological trait as a determining factor for *Populus simonii* Carr. to survive from drought in semi-arid region. *Agr. Water Manag.* 253, 106943.
- Lyu, S., Wang, J., Song, X., Wen, X., 2021. The relationship of δD and $\delta^{18}\text{O}$ in surface soil water and its implications for soil evaporation along grass transects of Tibet, Loess, and Inner Mongolia Plateau. *J. Hydrol.* 600, 126533.
- McDowell, N., Pockman, W.T., Allen, C.D., Breshears, D.D., Cobb, N., Kolb, T., Plaut, J., Sperry, J., West, A., Williams, D.G., et al., 2008. Mechanisms of plant survival and mortality during drought: why do some plants survive while others succumb to drought? *N. Phytol.* 178, 719–739.
- McVicar, T.R., Van Niel, T.G., Li, L., Wen, Z., Yang, Q., Li, R., Jiao, F., 2010. Parsimoniously modelling perennial vegetation suitability and identifying priority areas to support China's re-vegetation program in the Loess Plateau: matching model complexity to data availability. *Ecol. Manag.* 259, 1277–1290.
- Miguez-Macho, G., Fan, Y., 2021. Spatiotemporal origin of soil water taken up by vegetation. *Nature* 598, 624–628.
- Moore, J.W., Semmens, B.X., 2008. Incorporating uncertainty and prior information into stable isotope mixing models. *Ecol. Lett.* 11, 470–480.
- Moreno-Gutiérrez, C., Dawson, T.E., Nicolás, E., Querejeta, J.I., 2012. Isotopes reveal contrasting water use strategies among coexisting plant species in a Mediterranean ecosystem. *N. Phytol.* 196, 489–496.
- Orłowski, N., Winkler, A., McDonnell, J.J., Breuer, L., 2018. A simple greenhouse experiment to explore the effect of cryogenic water extraction for tracing plant source water. *Ecohydrology* 11, e1967.
- Prentice, I.C., Meng, T., Wang, H., Harrison, S.P., Ni, J., Wang, G., 2011. Evidence of a universal scaling relationship for leaf CO_2 drawdown along an aridity gradient. *N. Phytol.* 190, 169–180.
- Robertson, J.A., Gazis, C.A., 2006. An oxygen isotope study of seasonal trends in soil water fluxes at two sites along a climate gradient in Washington State (USA). *J. Hydrol.* 328, 375–387.
- Su, B., Shangguan, Z., 2019. Decline in soil moisture due to vegetation restoration on the Loess Plateau of China. *Land Degrad. Dev.* 30, 290–299.
- Sun, S., He, C., Qiu, L., Li, C., Zhang, J., Meng, P., 2018. Stable isotope analysis reveals prolonged drought stress in poplar plantation mortality of the Three-North Shelter Forest in Northern China. *Agr. . Meteorol.* 252, 39–48.
- Taneda, H., Sperry, J.S., 2008. A case-study of water transport in co-occurring ring-versus diffuse-porous trees: contrasts in water-status, conducting capacity, cavitation and vessel refilling. *Tree Physiol.* 28, 1641–1651.
- Tang, Y., Wu, X., Chen, Y., Wen, J., Xie, Y., Lu, S., 2018. Water use strategies for two dominant tree species in pure and mixed plantations of the semiarid Chinese Loess Plateau. *Ecohydrology* 11, e1943.
- Wang, J., Fu, B., Lu, N., Zhang, L., 2017. Seasonal variation in water uptake patterns of three plant species based on stable isotopes in the semi-arid Loess Plateau. *Sci. Total Environ.* 609, 27–37.
- Wang, J., Fu, B., Wang, L., Lu, N., Li, J., 2020. Water use characteristics of the common tree species in different plantation types in the Loess Plateau of China. *Agr. . Meteorol.* 288–289, 108020.
- Wang, J., Fu, B., Jiao, L., Lu, N., Li, J., Chen, W., Wang, L., 2021. Age-related water use characteristics of *Robinia pseudoacacia* on the Loess Plateau. *Agr. Meteorol.* 301–302.
- Wang, S., Fan, J., Ge, J., Wang, Q., Fu, W., 2019. Discrepancy in tree transpiration of *Salix matsudana*, *Populus simonii* under distinct soil, topography conditions in an ecological rehabilitation area on the Northern Loess Plateau. *Ecol. Manag.* 432, 675–685.
- Wen, M., Lu, Y., Li, M., He, D., Wei, X., Zhao, Y., Cui, B., Si, B., 2021. Correction of cryogenic vacuum extraction biases and potential effects on soil water isotopes application. *J. Hydrol.* 603, 127011.
- Wu, W., Tao, Z., Chen, G., Meng, T., Li, Y., Feng, H., Si, B., Manevski, K., Andersen, M.N., Siddique, K.H.M., 2022. Phenology determines water use strategies of three economic tree species in the semi-arid Loess Plateau of China. *Agr. . Meteorol.* 312, 108716.
- Xi, B., Clothier, B., Coleman, M., Duan, J., Hu, W., Li, D., Di, N., Liu, Y., Fu, J.Y., Li, J.S., et al., 2021. Irrigation management in poplar (*Populus* spp.) plantations: a review. *Ecol. Manag.* 494, 119330.
- Yamani, W.A., Green, S., Pangilinan, R., Dixon, S., Shahid, S.A., Kemp, P., Clothier, B., 2018. Water use of Al Ghaf (*Prosopis cineraria*) and Al Sidr (*Ziziphus spina-christi*) forests irrigated with saline groundwater in the hyper-arid deserts of Abu Dhabi. *Agr. Water Manag.* 203, 105–114.
- Yang, B., Dossa, G.G.O., Hu, Y.H., Liu, L.L., Meng, X.J., Du, Y.Y., Li, J.Y., Zhu, X.A., Zhang, Y.J., Singh, A.K., et al., 2023. Uncorrected soil water isotopes through cryogenic vacuum distillation may lead to a false estimation on plant water sources. *Methods Ecol. Evol.* 14, 1443–1456.
- Yang, X., Li, T., Shao, M., 2022. Factors controlling deep-profile soil organic carbon and water storage following *Robinia pseudoacacia* afforestation of the Loess Plateau in China. *. Ecosyst.* 9, 100079.
- Yang, Y., Fu, B., 2017. Soil water migration in the unsaturated zone of semiarid region in China from isotope evidence. *Hydrolog. Earth Syst. Sc.* 21, 1757–1767.
- Zhang, S., Yang, D., Yang, Y., Piao, S., Yang, H., Lei, H., Fu, B., 2018. Excessive afforestation and soil drying on China's Loess Plateau. *J. Geophys. Res. Biogeog.* 123, 923–935.
- Zhang, Z., Huang, M., Yang, Y., Zhao, X., 2020. Evaluating drought-induced mortality risk for *Robinia pseudoacacia* plantations along the precipitation gradient on the Chinese Loess Plateau. *Agr. Meteorol.* 284, 107897.
- Zhao, Y., Wang, L., 2021. Insights into the isotopic mismatch between bulk soil water and *Salix matsudana* Koidz trunk water from root water stable isotope measurements. *Hydrolog. Earth Syst. Sc.* 25, 3975–3989.
- Zhao, Y., Wang, L., Knighton, J., Evaristo, J., Wassen, M., 2021. Contrasting adaptive strategies by *Caragana korshinskii* and *Salix psammophila* in a semiarid revegetated ecosystem. *Agr. Meteorol.* 300, 108323.
- Zhao, Y., Dai, J., Tang, Y., Wang, L., 2022. Illuminating isotopic offset between bulk soil water and xylem water under different soil water conditions. *Agr. Meteorol.* 325, 109150.
- Zhou, J., Zhang, Z., Sun, G., Fang, X., Zha, T., McNulty, S., Chen, J., Jin, Y., Noormets, A., 2013. Response of ecosystem carbon fluxes to drought events in a poplar plantation in northern China. *Ecol. Manag.* 300, 33–42.